Theoretical Notes

Note 199

September 1974

SGEMP for Resonant Structures

K.S.H. Lee and L. Marin
Dikewood Corporation, Westwood Research Branch
Los Angeles, California

Abstract

Most satellites in existence to date are inherently resonant structures. By a resonant structure is meant that the currents and charges induced on it by an external transient electromagnetic source continue to oscillate without significant damping long after the external source has been turned off. In this note, the emphasis is on how important the resonance effects are on the system-generated EMP and how to calculate them.

The problem chosen for study is that of a thin cylindrical tube or a wire, which is a resonant structure, excited by a moving charged particle. The natural-mode method in conjunction with asymptotic expansion enables one to get an explicit analytical solution for the induced current on the wire. The solution is split into two parts: one part consists of damped sinusoids and the other has the quasi-static behavior. The analytical solution can be checked against the quasi-static solution as well as the numerical solution based on a space-time integral equation for the wire current. Such a check establishes ranges of validity and also numerical accuracy. For all practical purposes, the analytical solution deduced from the asymptotic natural-mode method is most desirable in predicting SGEMP for resonant structures.

Extensive graphical results for the time history of the induced wire currents are given. Explicit analytical expressions are obtained for the resonance frequencies, damping constants, and coupling coefficients of the current oscillations excited by a moving charge; these expressions are tabulated or graphed for ready use.

The results obtained in this note for a single charged particle can, in certain cases, be used as the Green's function for the problem of calculating the currents induced by many photoelectrons if all the nonlinear effects are neglected.

Table of Contents

		Page
Abstract		
Section		
I	Introduction	4
II	Quasi-Static Approach	7
III	Natural-Mode Method	15
IV	Space-Time Integral Formulation	39
V	Summary and Conclusion	49
Acknowledgement		50
References		51

Illustrations

Figure		Page
1	Photons impinging on a satellite.	5
2	A charge outside a wire.	8
3	New coordinates for the moving charge.	11
4	Normalized induced current for parallel motion.	13
5	Normalized induced current for perpendicular motion.	14
6	A charge moving parallel to a wire with constant velocity.	19
7	Contours for integration.	21
8a-8e	Variation of excitation coefficients with β.	29
9a-9e	Time history of induced current at the wire midpoint.	33
10a-10d	Comparison between natural-mode asymptotic solution and numerical solution for different Ω.	41
11a-11d	Comparison between the two solutions at higher velocity for different Ω.	45
12a-12b	Comparison between the two solutions for higher particle distance and different Ω.	47

I. Introduction

The photons released by an exoatmospheric nuclear detonation can travel great distances because of the absence of an intervening medium, i.e., the atmosphere. If a space communication system (for example, a satellite) happens to be above the atmosphere and along the line-of-sight path from the detonation point, the system will then be irradiated by a large amount of photons and consequently electrons will be ejected from the "surface" of the system by the photoelectric effect. Most electrons will return to the system and some will escape to infinity (see Fig. 1). Their motions near the system will create a transient electromagnetic field. Since this transient field is strongly dependent on the shape and constituents of the system, it has been appropriately referred to as the system-generated EMP [1,2]. The currents and charges induced on the system by this transient field may upset and/or damage the communication equipment inside the system.

Some past efforts [3,4] have been devoted to accurate calculations of the system-generated EMP (SGEMP) in which the system is modeled by a perfectly conducting sphere for reason of analytical tractability. The rigorous solution of that problem for orbital electron motions has provided invaluable physical insight and also led to the establishment of validity criteria for the quasi-static approach. It has been found that the criteria depend on the kinetic energies of the electrons as well as their distances from the sphere. Unless the electrons are very close to the sphere (such as less than one tenth the sphere's radius from the surface) the quasi-static solution is quite accurate for electron energies up to 2 MeV. The quasi-static approach to SGEMP boundary-value problems, if valid, is extremely desirable, since the physics involved in such an approach is less intricate and the mathematics is not as cumbersome as the corresponding dynamic approach. The success of the quasi-static approach to the sphere problem can be attributed to the fact that a sphere has large damping constants for all the exterior resonant modes that can be excited by the ejected electrons. For slender structures, however, the damping constants of the resonant modes are quite small and the quasi-static approach would not lead to accurate SGEMP predictions.

The present note treats one of the salient features of Fig. 1, i.e., the resonance effects of a slender structure on SGEMP. The simplest possible slender

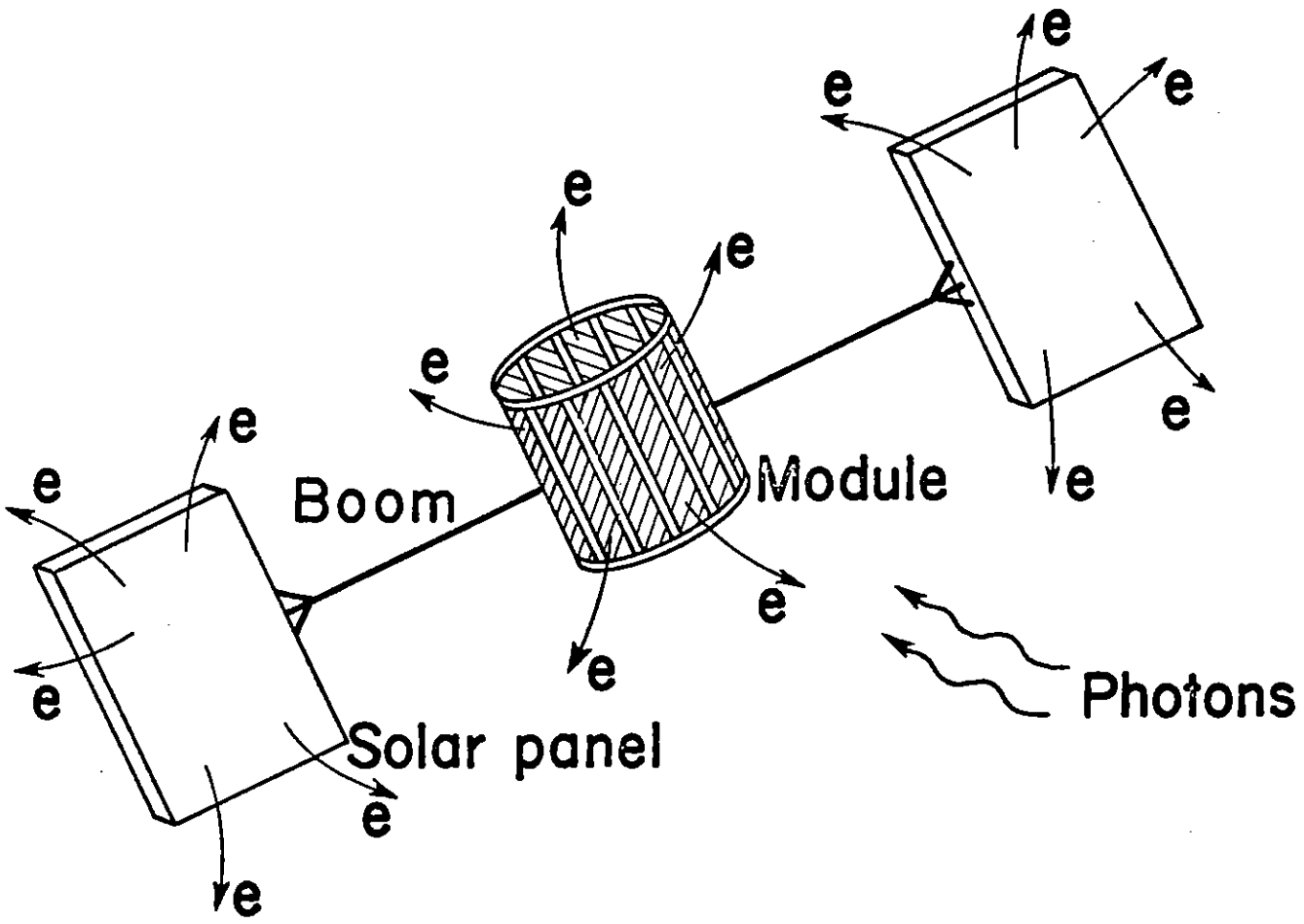

Figure 1. Photons impinging on a satellite.

structure is a straight thin wire. The boundary-value problem treated in this note is that of calculating the induced current on a straight thin wire by a moving charged particle with arbitrary prescribed trajectory. This problem, although geometrically quite simple, is not at all straightforward because the inducing field is quite complicated. By studying this problem in detail one will gain a thorough understanding of the resonance effects on the SGEMP-induced currents on a typical communication satellite. In a future study one may include other important features such as the solar panels and the module of Fig. 1.

In Section II, the quasi-static approach is used to find the induced current on a wire by moving charge. The natural-mode method (which is a part of SEM) is employed in Section III in order to place in evidence the resonances of the induced current. The natural frequencies and the associated modes are obtained explicitly by some suitable asymptotic expansion [5]. It turns out that the induced current can be written in an explicit form which can be split into two parts: one part consists of damped sinusoids and the other has the quasi-static behavior. Results are compared with those of Section II and, hence, validity criteria are established for the quasi-static approach. In Section IV, a space-time integral equation for the wire current is formulated and numerically solved by the method of characteristics. The numerical solution obtained here is then compared with that of the preceding section. The comparison shows that for a thin wire with $\Omega \geq 10$, the asymptotic solution is quite adequate for most practical purposes. In the fifth and final section results are summarized and conclusions drawn. Natural and desirable extensions to the present study are also suggested.

II. Quasi-Static Approach

In the quasi-static approach one first calculates the induced charge density on the wire surface by solving an appropriate electrostatic boundary-value problem. Then, by using the continuity equation the induced currents can be obtained from the induced charges.

Fig. 2 shows a particle with charge q located outside a perfectly conducting cylindrical tube with length ℓ and radius a. Let $\sigma(z,\phi)$ be the induced charge density on the tube. Then, on the surface of the tube the requirement that the total potential be constant gives

$$\frac{1}{4\pi\epsilon}\int_0^{\ell}\int_0^{2\pi}\frac{\sigma(z',\phi')a\,d\phi'dz'}{\sqrt{2a^2-2a^2\cos(\phi-\phi')+(z-z')^2}}+\frac{q}{4\pi\epsilon R}=V_o \tag{1}$$

where V_o is a constant (the induced potential on the tube), $R^2=a^2+\rho_o^2-2\rho_o a\cos(\phi-\phi_o)+(z-z_o)^2$, and (ρ_o,ϕ_o,z_o) denotes the location of the particle. The constraint on σ is that

$$\int_0^{\ell}\int_0^{2\pi}\sigma(z',\phi')a\,d\phi'dz'=-q \tag{2}$$

implying that the charged particle comes off from the tube. Averaging (1) with respect to ϕ one gets

$$\frac{1}{2\pi}\int_0^{2\pi}d\phi\int_0^{\ell}\frac{\tau(z')dz'}{\sqrt{2a^2-2a^2\cos\phi+(z-z')^2}}+\frac{q}{2\pi}\int_0^{2\pi}\frac{d\phi}{\sqrt{a^2+\rho_o^2-2\rho_o a\cos\phi+(z-z_o)^2}}=4\pi\epsilon V_o \tag{3}$$

where the line charge density τ is defined as

$$\tau(z)=\int_0^{2\pi}\sigma(z,\phi)a\,d\phi\,. \tag{4}$$

When the tube is thin ($\ell \gg a$) (a thin tube will simply be referred to as a wire hereafter), (3) can be solved approximately by using the fact that [6], if $z \neq 0,\ell$,

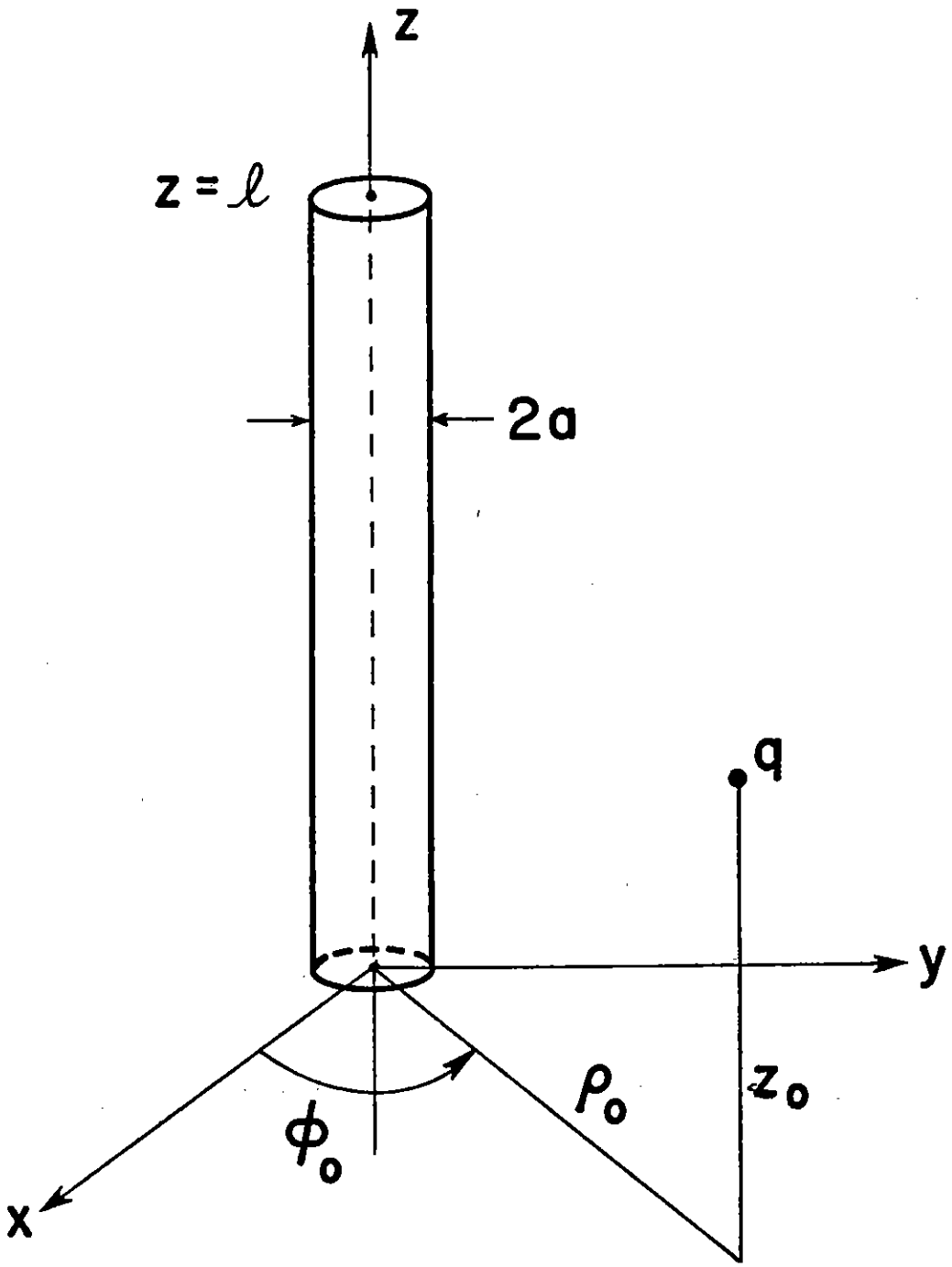

Figure 2. A charge outside a wire

$$\frac{1}{2\pi}\int_0^{2\pi}\int_0^{\ell}\frac{dz'd\phi}{\sqrt{2a^2-2a^2\cos\phi+(z-z')^2}} \approx 2\log\left(\frac{\ell}{a}\right)\equiv \Omega. \tag{5}$$

Hence, if $\Omega >> 1$ the approximate solution of (3) is

$$\tau(z) = \frac{4\pi\varepsilon}{\Omega} V_o - \frac{q}{\Omega\sqrt{\rho_o^2+(z-z_o)^2}}. \tag{6}$$

By applying the constraint (2) to (6) the constant V_o is found to be

$$V_o = \frac{q}{4\pi\varepsilon\ell}\left[\log\frac{(\ell-z_o)+\sqrt{(\ell-z_o)^2+\rho_o^2}}{\sqrt{\rho_o^2+z_o^2}-z_o} - \Omega\right] \tag{7}$$

which gives the voltage induced on the wire by the charge q.

The induced total current I_s (where the subscript s reminds one of the quasi-static approximation) is related to the line charge density τ by the continuity equation

$$\frac{\partial I_s}{\partial z} = -\frac{\partial\tau}{\partial t} \equiv \dot{\tau}. \tag{8}$$

Integrating (8) with τ given by (6) one obtains

$$\begin{aligned} I_s(z,t) &= -\frac{\partial}{\partial t}\int_0^z \tau(z')dz' \\ &= \frac{q}{\Omega\ell}\frac{\partial}{\partial t}\left[\ell\log\frac{(z-z_o)+\sqrt{(z-z_o)^2+\rho_o^2}}{\sqrt{z_o^2+\rho_o^2}-z_o} - z\log\frac{(\ell-z_o)+\sqrt{(\ell-z_o)^2+\rho_o^2}}{\sqrt{z_o^2+\rho_o^2}-z_o}\right] \end{aligned} \tag{9}$$

where $z_o = z_o(t)$, $\rho_o = \rho_o(t)$, i.e., the position of the charge is taken to be a function of time. It is easy to see from (9) that

$$I_s(0,t) = I_s(\ell,t) = 0 \tag{10}$$

as they should.

To carry out the time differentiation in (9) it is more expedient to use the coordinates as shown in Fig. 3. With respect to these coordinates one has, for example,

$$\frac{\sqrt{(z-z_o)^2+\rho_o^2}+z-z_o}{\sqrt{\rho_o^2+z_o^2}-z_o} = \frac{r(1-\cos\theta)}{r_o(1-\cos\theta_o)} = \frac{r_o(\sin\theta_o/\sin\theta)\sin^2(\theta/2)}{r_o\sin^2(\theta_o/2)}$$

$$= \cot(\theta_o/2)\tan(\theta/2).$$

Thus, (9) can be rewritten as

$$I_s(z,t) = \frac{q}{\Omega\ell}\frac{\partial}{\partial t}\left\{\ell\log[\tan(\theta/2)\cot(\theta_o/2)] - z\log[\tan(\theta_\ell/2)\cot(\theta_o/2)]\right\}$$

$$= \frac{q}{\Omega\ell\rho_o}\left[(z-\ell)r_o\dot{\theta}_o + \ell r\dot{\theta} - zr_\ell\dot{\theta}_\ell\right]. \tag{11}$$

Let the particle's velocity $\underline{v}$ be decomposed into components parallel and perpendicular to the axis of the wire, i.e.,

$$\underline{v} = \underline{e}_z v_{\parallel} + \underline{e}_\rho v_{\perp}.$$

Some manipulations of (11) then give

$$I_s(z,t) = \frac{qv_{\parallel}}{\Omega\rho_o}\left[(1-\frac{z}{\ell})\sin\theta_o - \sin\theta + \frac{z}{\ell}\sin\theta_\ell\right]$$

$$- \frac{qv_{\perp}}{\Omega\rho_o}\left[(1-\frac{z}{\ell})\cos\theta_o - \cos\theta + \frac{z}{\ell}\cos\theta_\ell\right]. \tag{12}$$

When the charged particle is very close to the wire, the current right beneath the particle is given by

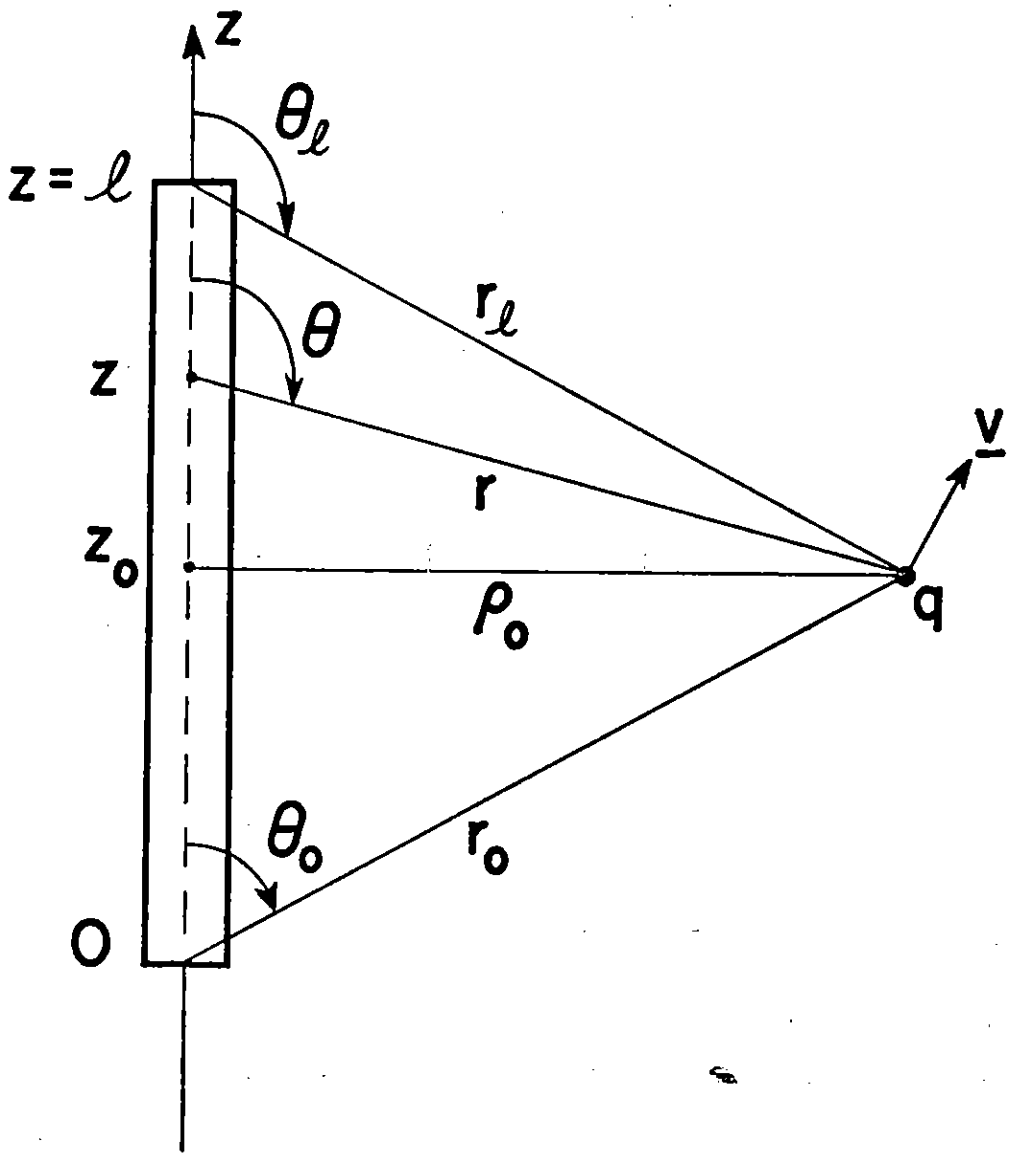

Figure 3. New coordinates for the moving charge.

$$I_s(z_o,t) \approx -\frac{qv_{\parallel}}{\Omega\rho_o} - \frac{qv_{\perp}}{\Omega\rho_o}\left(1 - \frac{2z_o}{\ell}\right) \tag{13}$$

which has been obtained from (12) by letting $\theta = \pi/2$, $\theta_o \approx 0$, $\theta_\ell \approx \pi$. Thus, the current varies in inverse proportion to the distance of the charge from the wire axis.

When (12) is evaluated at the midpoint of the wire $(z = \ell/2)$ where one can expect large currents on physical grounds, one gets

$$I_s(\ell/2,t) = -\frac{qv_{\parallel}}{2\Omega}\left(\frac{2}{r} - \frac{1}{r_o} - \frac{1}{r_\ell}\right)$$

$$-\frac{qv_{\perp}}{2\Omega\rho_o}\left(\frac{\ell-2z_o}{r} + \frac{z_o}{r_o} - \frac{\ell-z_o}{r_\ell}\right). \tag{14}$$

In terms of the dimensionless variables ξ and η defined as

$$\xi = \frac{z_o}{\ell} = \frac{vt}{\ell}, \qquad \eta = \frac{\rho_o}{\ell} \tag{15}$$

one can rewrite (14) as

$$I_s(\ell/2,t) = -\frac{qv_{\parallel}}{2\Omega\ell}\,\bar{I}_{\parallel} - \frac{qv_{\perp}}{2\Omega\ell}\,\bar{I}_{\perp}$$

$$\bar{I}_{\parallel} = \frac{2}{\sqrt{\eta^2+(\tfrac{1}{2}-\xi)^2}} - \frac{1}{\sqrt{\eta^2+\xi^2}} - \frac{1}{\sqrt{\eta^2+(1-\xi)^2}} \tag{16}$$

$$\bar{I}_{\perp} = \frac{1}{\eta}\left[\frac{2(\tfrac{1}{2}-\xi)}{\sqrt{\eta^2+(\tfrac{1}{2}-\xi)^2}} + \frac{\xi}{\sqrt{\eta^2+\xi^2}} - \frac{1-\xi}{\sqrt{\eta^2+(1-\xi)^2}}\right].$$

According to (15) the time origin $(t = 0)$ is chosen to be the instant when the particle is right above one end $(z = 0)$ of the wire. The normalized current components, $\bar{I}_{\parallel}$ and $\bar{I}_{\perp}$, are plotted in Figs. 4 and 5 from which one can obtain the induced current at the midpoint of the wire in terms of the instantaneous position (ξ,η) of the charged particle.

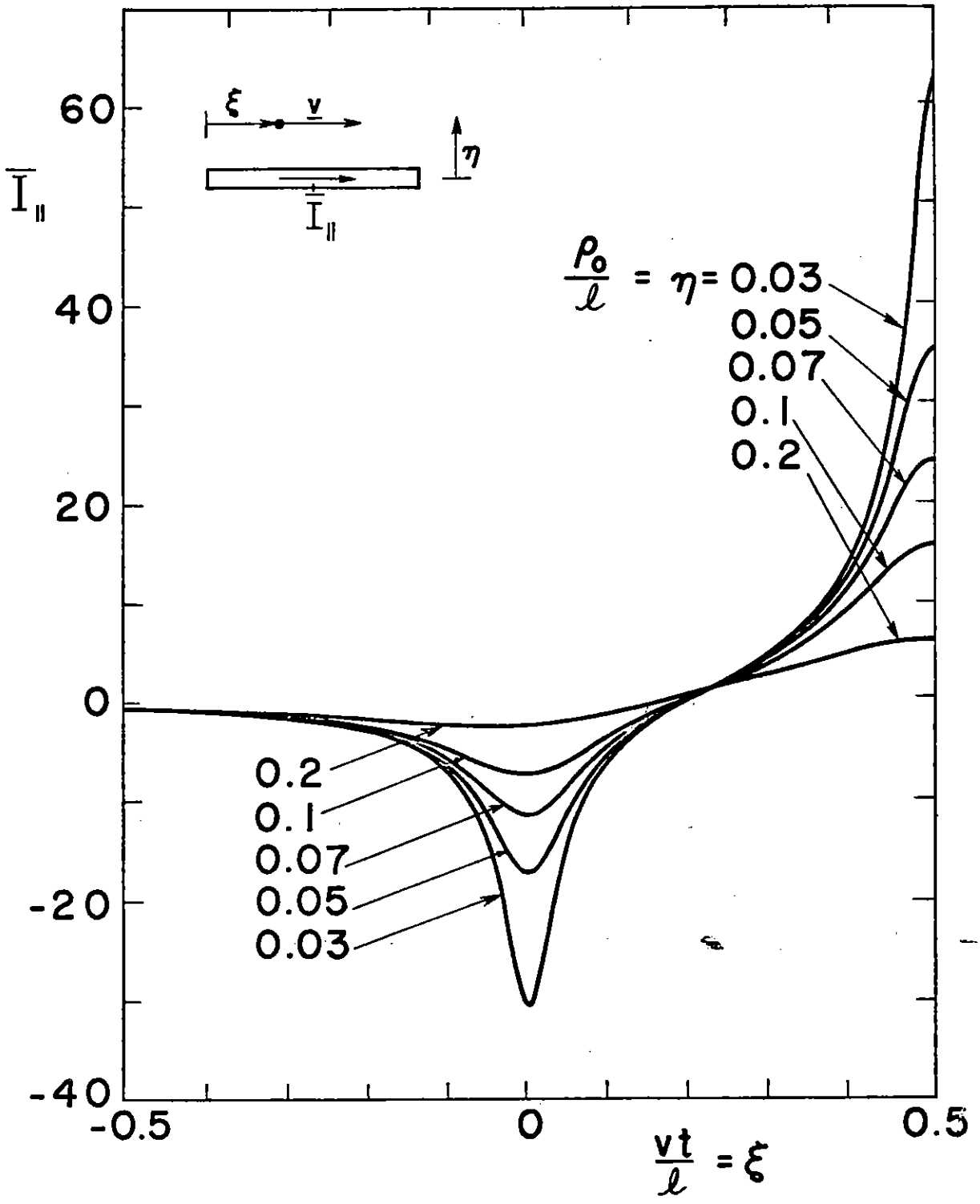

Figure 4. Normalized induced current for parallel motion.

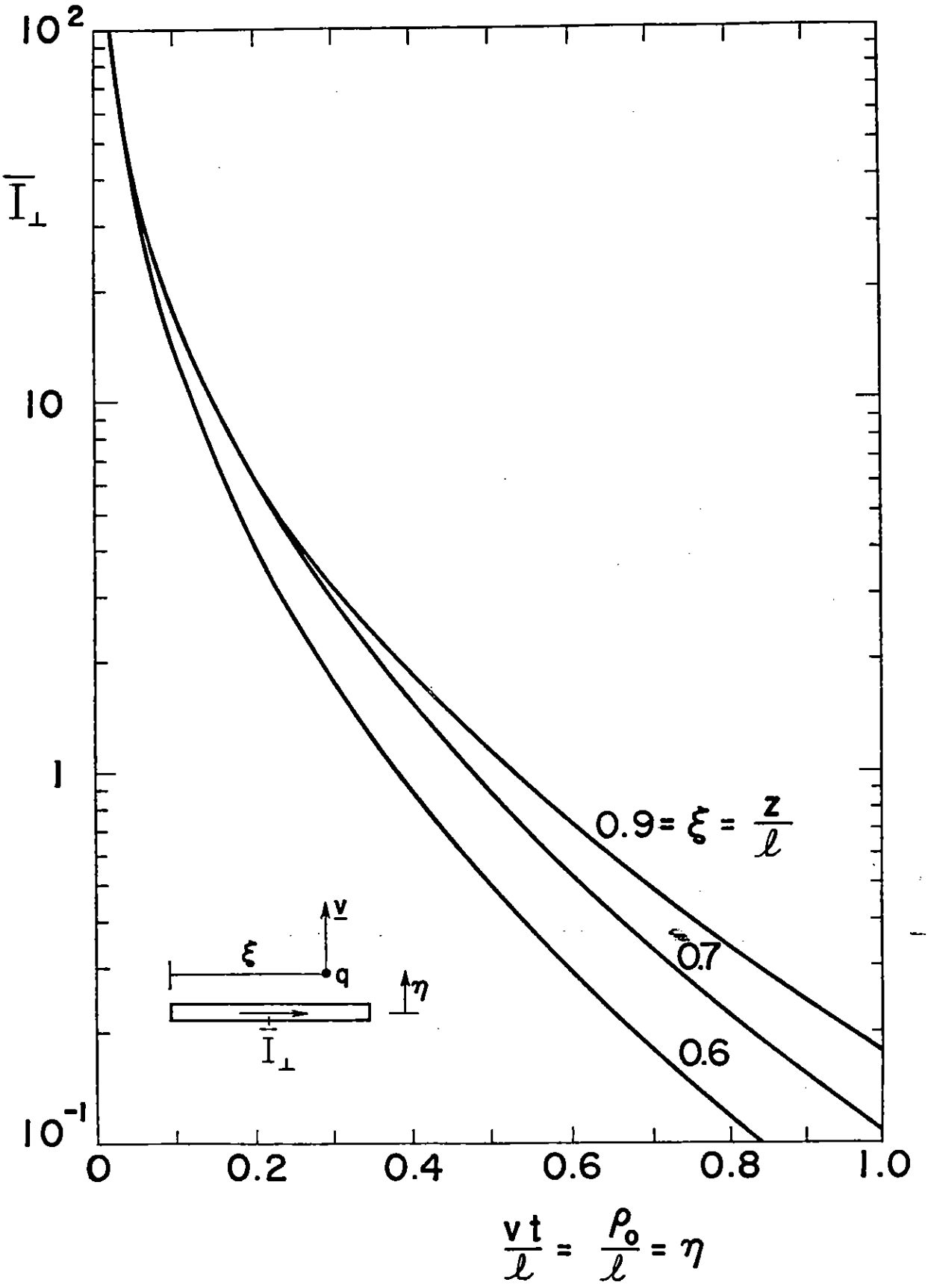

Figure 5. Normalized induced current for perpendicular motion.

III. Natural-Mode Method

In the quasi-static approach presented in the last section any resonances that are inherent in a thin wire are neglected from the outset. In this section the effect of these resonances on the wire current induced by a moving charged particle will be examined in detail.

The point of departure is the well-known integro-differential equation for the current I in the s-domain:

$$\left(\frac{d^2}{dz^2} - \frac{s^2}{c^2}\right)\int_0^{\ell} \frac{I(z',s)}{4\pi R}\, e^{-sR/c}\, dz' = -s\varepsilon E_z^{inc}(z,s) \tag{17}$$

where $R^2 = (z - z')^2 + a^2$, i.e., the so-called thin-wire approximation has been used. Here, it should be pointed out that in the asymptotic method employed in the last as well as this section, one could have used the exact kernel in (17), and the final result will however be the same as that derived from the thin-wire approximation.

From the method of singularity expansion (SEM) the solution of (17) can be written as [5,7]

$$I(z,s) = -\varepsilon s \sum_n \frac{1}{s-s_n} \frac{C_n}{B_n} I_n(z). \tag{18}$$

For a thin wire it has been found that [5,8]

$$\begin{aligned}
I_n(z) &= \sin\frac{n\pi z}{\ell} + O\left(\frac{1}{\Omega}\right) \\
s_n &= \pm\frac{in\pi c}{\ell} - \frac{c}{\Omega\ell}\left[\gamma + \ln(2n\pi) - Ci(2n\pi) \pm iSi(2n\pi)\right] + O\left(\frac{1}{\Omega^2}\right) \\
&\qquad \gamma = 0.577\cdots \text{ (Euler's constant)} \\
C_n &= \int_0^{\ell} \sin\left(\frac{n\pi z}{\ell}\right) E_z^{inc}(z,s)dz + O\left(\frac{1}{\Omega}\right) \\
B_n &= \int_0^{\ell}\left[\left(\frac{d\mathcal{L}}{ds}\right)_{s_n} I_n\right] I_n(z)dz \\
&= -\Omega\frac{\ell s_n}{4\pi c^2} + O(1)
\end{aligned} \tag{19}$$

where $\Omega = 2\log(\ell/a)$, $Ci(x)$ and $Si(x)$ are respectively the cosine and sine integrals, and $\mathcal{L}$ denotes the integro-differential operator that operates on the current I in (17). Substitution of (19) in (18) gives, with Z_o denoting the free-space impedance,

$$I(z,s) = \frac{4\pi c}{Z_o \Omega \ell} \sum_n \frac{s}{s_n(s-s_n)} \left[\int_0^\ell \sin(n\pi z'/\ell) E_z^{inc}(z',s)dz'\right] \sin(n\pi z/\ell) + O\left(\frac{1}{\Omega^2}\right). \quad (20)$$

Here, one may notice that coupling coefficients of "class 2" have been used, i.e., they are allowed to be functions of s [7]. The reason for such a choice is that in the low-frequency limit, (20) directly leads to the quasi-static solution of last section. If one had used coupling coefficients of "class 1", entire functions would have to be introduced in order to have exact correspondance with the quasi-static solution. To see how (20) reduces to the quasi-static solution (9) when $s \to 0$ one lets $s_n = \pm in\pi c/\ell$ $(n > 0)$ in (20) and obtains

$$I(z,s) \approx \frac{8\pi cs}{Z_o \Omega \ell} \int_0^\ell E_z^{inc}(z',s)dz' \sum_{n>0} \frac{\sin(n\pi z/\ell)\sin(n\pi z'/\ell)}{s^2+(n\pi/\ell)^2}. \quad (21)$$

The series, after dropping the s^2 term, can be summed as [9]

$$\sum_{n>0} \frac{\sin(n\pi z/\ell)\sin(n\pi z'/\ell)}{(n\pi/\ell)^2} = \begin{cases} (\ell - z)z'/2, & z > z' \\ (\ell - z')z/2, & z < z'. \end{cases} \quad (22)$$

Thus, (21) becomes

$$I(z,s) \approx \frac{4\pi\epsilon s}{\Omega} \left[\int_0^z z'(1 - z/\ell)E_z^{inc}(z',s)dz' + \int_z^\ell z(1 - z'/\ell)E_z^{inc}(z',s)dz'\right] \quad (23)$$

whence

$$I(z,t) \approx \frac{4\pi\epsilon}{\Omega} \frac{d}{dt} \left[\int_0^z z'(1 - z/\ell)E_z^{inc}(z',t)dz' + \int_z^\ell z(1 - z'/\ell)E_z^{inc}(z',t)dz'\right]. \quad (24)$$

Using the Coulomb field for E_z^{inc} and evaluating the integrals one gets the quasi-static expression (9).

There is another interesting thing about expression (21). It is in fact the solution of the differential equation

$$\left(\frac{d^2}{dz^2} - \frac{s^2}{c^2}\right) I = -\frac{4\pi}{\Omega} s\epsilon E_z^{inc} \tag{25}$$

with the boundary conditions $I(0,s) = I(\ell,s) = 0$. This equation can be solved by use of the Green's function

$$G(z,z') = \frac{2}{\ell} \sum_{n>0} \frac{\sin(n\pi z/\ell)\sin(n\pi z'/\ell)}{s^2+(n\pi/\ell)^2}$$

which satisfies the differential equation

$$\left(\frac{d^2}{dz^2} - \frac{s^2}{c^2}\right) G = -\delta(z - z')$$

and the boundary conditions $G(0,z') = G(\ell,z') = 0$. It has to be emphasized, however, that (25) together with the zero boundary conditions gives only undamped oscillations which are exactly the same as those given by (20) provided that the radiation damping is neglected.

Turning back to (20), taking its inverse Laplace transform, and dropping the $O(\Omega^{-2})$ term one obtains the induced current in the time domain, viz.,

$$I(z,t) = \frac{4\pi c}{Z_o \Omega \ell} \sum_n \left[\frac{1}{s_n} \int_{-\infty}^{t} dt' \, e^{s_n(t-t')} \int_0^{\ell} \sin(n\pi z'/\ell) \frac{\partial}{\partial t'} E_z^{inc}(z',t')dz'\right] \sin(n\pi z/\ell). \tag{26}$$

Integration by parts yields

$$I(z,t) = -\frac{4\pi c}{Z_o \Omega \ell} \sum_n \left[\frac{1}{s_n^2} \int_0^{\ell} \sin(n\pi z'/\ell) \frac{\partial}{\partial t} E_z^{inc}(z',t)dz'\right] \sin(n\pi z/\ell)$$

$$+ \frac{4\pi c}{Z_o \Omega \ell} \sum_n \left[\frac{1}{s_n^2} \int_{-\infty}^{t} dt' \, e^{s_n(t-t')} \int_0^{\ell} \sin(n\pi z'/\ell) \frac{\partial^2}{\partial t'^2} E_z^{inc}(z',t')dz'\right] \sin(n\pi z/\ell). \tag{27}$$

Since E_z^{inc} is due to a moving charge, it is clear that each time differentiation of this quantity brings in a multiplicative factor v/c. Thus, the continuous process of integrating (27) by parts amounts to developing a power series in v/c. Unfortunately, there is no particular advantage of doing this because it is difficult to evaluate all the integrals involved in the coefficients of such a series. Nevertheless, expression (27) is physically appealing. The first sum can be shown, by means of (22), to reduce to the quasi-static solution (9) when damping is neglected. The second sum, of course, represents the transient oscillations.

Up to now the discussions have been for any general incident field. Here and in the following, the incident field will be specified as that of a point charge moving with a constant speed and parallel to the axis of the wire. Even such a simple motion for the charge would require complicated mathematical manipulations for the determination of the induced wire current, as will be seen below. The electric field of a moving charge along the wire axis is given by [10]

$$E_z^{inc}(z,t) = -\frac{q}{4\pi\varepsilon}\frac{\gamma(vt-z)}{[\rho_o^2+\gamma^2(vt-z)^2]^{3/2}} \tag{28}$$

where $\gamma = (1-\beta^2)^{-1/2}$, $\beta = v/c$, and ρ_o is the transverse distance of the charge from the wire axis (see Fig. 6). As before, $t = 0$ is defined to be the instant when the charge is right above one end $(z = 0)$ of the wire. Since an infinite path is being considered, it is more convenient to talk about Fourier than Laplace transforms. The Fourier transform of (28) gives [11]

$$\begin{aligned} E_z^{inc}(z,\omega) &= -\frac{q}{4\pi\varepsilon}\int_{-\infty}^{\infty}\frac{\gamma(vt-z)}{[\rho_o^2+\gamma^2(vt-z)^2]^{3/2}}e^{i\omega t}\,dt \\ &= -\frac{iq}{2\pi\varepsilon}\frac{e^{i\omega z/v}}{\gamma v\rho_o}\int_0^{\infty}x(1+x^2)^{-3/2}\sin[\rho_o\omega x/(\gamma v)]\,dx \\ &= \begin{cases} -\dfrac{iq}{2\pi\varepsilon}\dfrac{e^{i\omega z/v}}{\gamma v\rho_o}\dfrac{\rho_o\omega}{\gamma v}K_o[\rho_o\omega/(\gamma v)], & \omega > 0 \\ -\dfrac{iq}{2\pi\varepsilon}\dfrac{e^{i\omega z/v}}{\gamma v\rho_o}\dfrac{\rho_o\omega}{\gamma v}K_o[-\rho_o\omega/(\gamma v)], & \omega < 0. \end{cases} \end{aligned} \tag{29}$$

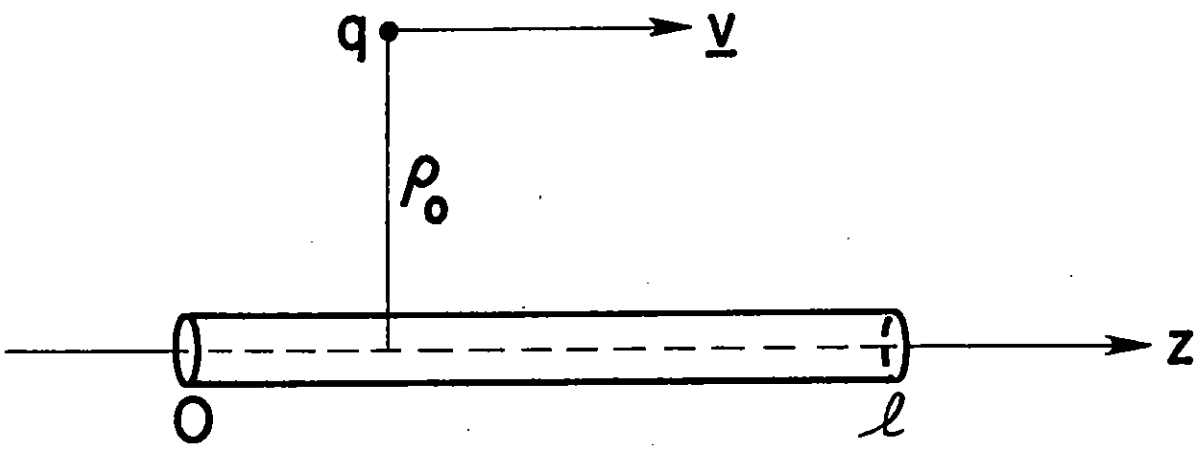

Figure 6. A charge moving parallel to a wire with constant velocity.

It should be noted that the modified Bessel function K_o has to be defined for negative argument as is indicated in (29), so that the inverse Fourier transform of $E_z^{inc}(z,\omega)$ gives back (28).

When one substitutes (28) in either (26) or (27), it is easy to see that these two expressions are not particularly suitable for numerical computation. To this end let the coefficient C_n in (20) be first evaluated with E_z^{inc} given by (29). Thus,

$$C_n = \int_0^{\ell} E_z^{inc}(z,\omega)\sin(n\pi z/\ell)dz$$

$$= -\frac{iq}{2\pi\epsilon}\frac{\omega}{\gamma^2 v^2} K_o[\rho_o\omega/(\gamma v)]\ \frac{n\pi/\ell}{(n\pi/\ell)^2-(\omega/v)^2}\left[1 - (-)^n e^{i\omega\ell/v}\right], \quad \text{Re } \omega > 0. \quad (30)$$

Here, the expression (29) for the incident field has been entended to complex values of ω. For Re $\omega < 0$, one simply replaces $K_o(\rho_o\omega/\gamma v)$ by $K_o(-\rho_o\omega/\gamma v)$ in (30). Using (30) and setting $s = -i\omega$ in (20) one obtains

$$I_{\parallel}(z,\omega)$$

$$= \frac{2q}{\Omega\ell\gamma^2}\omega^2 K_o[\rho_o\omega/(\gamma v)]\ \sum_n \frac{1}{\omega_n(\omega-\omega_n)}\ \frac{n\pi/\ell}{(n\pi\beta/\ell)^2-(\omega/c)^2}\left[1 - (-)^n e^{i\omega\ell/v}\right]\sin(n\pi z/\ell)$$

$$\text{Re } \omega > 0 \quad (31)$$

and

$$I_{\parallel}(z,t) = \frac{1}{2\pi}\int_C I_{\parallel}(z,\omega)e^{-i\omega t}\, d\omega \quad (32)$$

where, as shown in Fig. 7 , the contour C is above all SEM poles of $I(z,\omega)$ and the branch cuts are drawn according to the definition of K_o discussed in connection with (30). By deforming C appropriately for different time intervals one can obtain various forms suitable for numerical computation.

(a) $t < 0$

For $t < 0$ one deforms C into C_1 and C_∞ (Fig. 7). It is easily

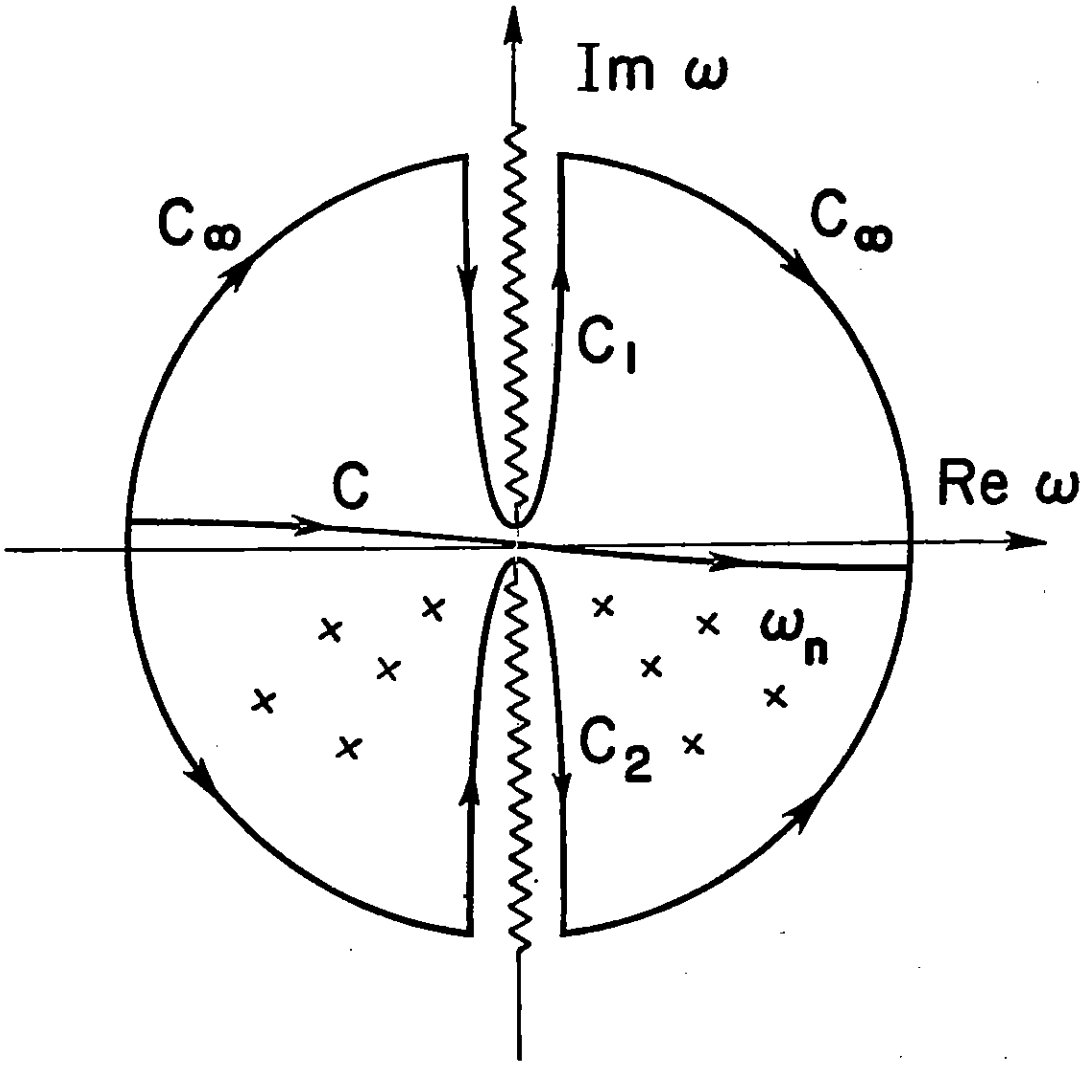

Figure 7. Contours for integration.

seen that the integral along C_∞ vanishes. Thus, (32) becomes, after some manipulations,

$$I_{\parallel}(z,t) = \frac{1}{2\pi}\int_{C_1} I_{\parallel}(z,\omega)e^{-i\omega t}\,d\omega$$

$$= \frac{2\pi qv}{\Omega\ell\gamma^2}\sum_{n>0} n\sin(n\pi z/\ell)\int_0^\infty \frac{x^2}{\beta^2x^2+\pi^2}\,\frac{1-(-)^n e^{-x}}{x^2+n^2\pi^2}\,J_o(\eta x/\gamma)e^{x\xi}\,dx, \quad \xi < 0 \qquad (33)$$

where, as in Section II, $\eta = \rho_o/\ell$, $\xi = vt/\ell$. Using, first, partial fractions and then the fact that series like

$$\sum_{n=1}^{\infty}\frac{n\sin nx}{n^2+a^2} \quad \text{and} \quad \sum_{n=1}^{\infty}\frac{(-)^n n\sin nx}{n^2+a^2}$$

can be summed in closed form [9] one obtains from (33)

$$I_{\parallel}(z,t) = \frac{qv}{\Omega\ell}\int_0^\infty\left[\frac{\sinh\{(1-z/\ell)\beta x\}}{\sinh\beta x} + e^{-x}\,\frac{\sinh(\beta xz/\ell)}{\sinh\beta x} - \frac{\sinh\{(1-z/\ell)x\}}{\sinh x}\right.$$

$$\left. - e^{-x}\,\frac{\sinh(xz/\ell)}{\sinh x}\right]J_o(\eta x/\gamma)e^{\xi x}\,dx, \qquad \xi < 0. \qquad (34)$$

At the midpoint $(z = \ell/2)$ of the wire (34) gives

$$I_{\parallel}(\ell/2,t) = -\frac{qv}{\Omega\ell}\,\frac{1}{\sqrt{(\eta/\gamma)^2+(\xi-1/2)^2}} + \frac{qv}{2\Omega\ell}\int_0^\infty \frac{e^{-|\xi|x}+e^{-|1-\xi|x}}{\cosh(\beta x/2)}\,J_o(\eta x/\gamma)\,dx \qquad (35)$$

$$\equiv -\frac{qv}{2\Omega\ell}\,F(\xi,\eta;\beta), \qquad \xi < 0 \qquad (t < 0).$$

Expanding (35) in a power series in β one gets

$$I_{\parallel}(\ell/2,t) = -\frac{qv}{2\Omega\ell}F(\xi,\eta;\beta) = -\frac{qv}{2\Omega\ell}\left[\frac{2}{\sqrt{\eta^2+(\xi-1/2)^2}} - \frac{1}{\sqrt{\eta^2+\xi^2}} - \frac{1}{\sqrt{\eta^2+(1-\xi)^2}}\right]$$

$$- \frac{qv}{2\Omega\ell}\left[\frac{\eta^2}{[\eta^2+(\xi-1/2)^2]^{3/2}} - \frac{5\eta^2+2\xi^2}{8(\eta^2+\xi^2)^{5/2}}\right.$$

$$\left. - \frac{5\eta^2+2(\xi-1)^2}{8[\eta^2+(\xi-1)^2]^{5/2}}\right]\beta^2 + \frac{qv}{2\Omega\ell}O(\beta^4). \qquad (36)$$

Here, one notices that the first term is exactly the quasi-static solution given by (16). By examining the second term, i.e., the correction term, in (36) one can conclude that the quasi-static solution is good if

$$\eta^2 + \xi^2 > \beta^2 \quad \text{and} \quad \eta^2 + (\xi - 1)^2 > \beta^2$$

(b) $0 < t < \ell/v$

During this time interval the charge is moving right above the wire. To evaluate the inverse Fourier transform integral (32) one deforms C into C_1 (Fig. 7) for the exponential factor $\exp[i\omega(\ell/v - t)]$, and C into C_2 for the exponential factor $\exp(-i\omega t)$. After some lengthy but straightforward manipulations, one can reduce (32) to

$$I_{\parallel}(z,t) = \frac{qv}{\Omega\ell}\int_0^\infty \left[\frac{\sinh(\beta xz/\ell)}{\sinh \beta x} - \frac{\sinh(xz/\ell)}{\sinh x}\right] J_o(\eta x/\gamma)e^{-(1-\xi)x}\,dx$$

$$+ \frac{qv}{\Omega\ell}\int_0^\infty \left[\frac{\sinh\{(1-z/\ell)\beta x\}}{\sinh \beta x} - \frac{\sinh\{(1-z/\ell)x\}}{\sinh x}\right] J_o(\eta x/\gamma)e^{-\xi x}\,dx \qquad (37)$$

$$- 2\pi i \sum(\text{Residues}), \qquad 0 < \xi < 1.$$

As evident from expression (31), the residues are associated with two different kinds of poles: the poles ω_n of the natural modes and the poles $n\pi v/\ell$ of the particle's field. Summing all these residues one has

$$-2\pi i \sum(\text{Residues}) = \frac{4qc}{\Omega\ell} \sum_{n>0} K_o[n\pi\eta/(\gamma\beta)]e^{-\alpha_n t} \sin(n\pi ct/\ell - \beta_n t)\sin(n\pi z/\ell)$$

$$- \frac{4qv}{\Omega\ell} \sum_{n>0} K_o(n\pi\eta/\gamma)\sin(n\pi\xi)\sin(n\pi z/\ell) \qquad (38)$$

where

$$\alpha_n = -\text{Re } s_n = \frac{c}{\Omega\ell}\,[0.577\cdots + \ln(2n\pi) - \text{Ci}(2n\pi)]$$

$$\beta_n = -\text{Im } s_n = \frac{c}{\Omega\ell}\,\text{Si}(2n\pi).$$

Evaluation of (37) at the midpoint $(z = \ell/2)$ of the wire gives

$$I_{\parallel}(\ell/2,t) = \frac{4qc}{\Omega\ell} \sum_{n=1,3,5\cdots} (-)^{(n-1)/2} K_o[n\pi\eta/(\gamma\beta)]e^{-\alpha_n t} \sin(n\pi ct/\ell - \beta_n t)$$

$$- \frac{2qv}{\Omega\ell} \sum_{n>0} K_o(n\pi\eta/\gamma)[\cos n\pi(\xi - 1/2) - \cos n\pi(\xi + 1/2)] \qquad (39)$$

$$+ \frac{qv}{2\Omega\ell} \int_0^\infty \left[\frac{e^{-\xi x}+e^{-(1-\xi)x}}{\cosh(\beta x/2)} - \frac{e^{-\xi x}+e^{-(1-\xi)x}}{\cosh(x/2)}\right] J_o(\eta x/\gamma)dx, \quad 0 < \xi < 1.$$

The second sum will now be shown to cancel part of the integral in (39). First, one has

$$\int_0^\infty \frac{e^{-\xi x}+e^{-(1-\xi)x}}{\cosh(x/2)}\, J_o(\eta x/\gamma)dx$$

$$= 2\int_0^\infty \sum_{n=0}^\infty (-)^n \left\{e^{-(n+\xi+1/2)x} + e^{-(n-\xi+3/2)x}\right\} J_o(\eta x/\gamma)dx$$

$$= -2\sum_{n=1}^\infty (-)^n \left\{[(\eta/\gamma)^2 + (n - \xi + 1/2)^2]^{-1/2} - [(\eta/\gamma)^2 + (n + \xi + 1/2)^2]^{-1/2}\right\}$$

$$+ \frac{2}{\sqrt{(\eta/\gamma)^2+(\xi+1/2)^2}}\,.$$

From Ref. [9] one has

$$\sum_{n>0} K_o(n\pi\eta/\gamma)\{\cos[n\pi(\xi - 1/2)] - \cos[n\pi(\xi + 1/2)]\}$$

$$= \frac{1}{2}\left[\frac{1}{\sqrt{(\eta/\gamma)^2+(\xi-1/2)^2}} - \frac{1}{\sqrt{(\eta/\gamma)^2+(\xi+1/2)^2}}\right]$$

$$+ \frac{1}{2}\sum_{n=1}^{\infty}(-)^n\left\{[(\eta/\gamma)^2 + (n - \xi + 1/2)^2]^{-1/2} - [(\eta/\gamma)^2 + (n + \xi + 1/2)^2]^{-1/2}\right\}.$$

Thus, (39) is simplified to

$$I_{\parallel}(\ell/2,t) = \frac{4qc}{\Omega\ell}\sum_{n=1,3,5\cdots}(-)^{(n-1)/2} K_o[n\pi\eta/(\gamma\beta)]e^{-\alpha_n t}\sin(n\pi ct/\ell - \beta_n t)$$

$$- \frac{qv}{2\Omega\ell}F(\xi,\eta;\beta), \qquad 0 < \xi < 1 \quad (0 < t < \ell/v) \qquad (40)$$

where F is given by (35).

(c) $t > \ell/v$

During this time interval the particle has passed the wire and continues to move away from the wire. To evaluate the inverse Fourier transform integral (32) for $t > \ell/v$ one deforms C into C_2 (Fig. 7) and obtains

$$I_{\parallel}(z,t) = \frac{2\pi qv}{\Omega\ell\gamma^2}\sum_{n>0} n\sin(n\pi z/\ell)\int_0^{\infty}\frac{x^2}{\beta^2x^2+n^2\pi^2}\frac{1-(-)^n e^x}{x^2+n^2\pi^2}J_o(\eta x/\gamma)e^{-\xi x}\,dx$$

$$- 2\pi i\sum(\text{Residues}), \qquad \xi > 1. \qquad (41)$$

One can easily observe that the first sum is equal to (33) if one interprets ξ in (33) to be $1 - \xi$ in (41) and that the residue series is due only to the poles of the natural modes since the residue at $n\pi v/\ell$ is zero. Hence, at the

midpoint $(z = \ell/2)$ of the wire (41) is reduced to

$$I(\ell/2,t) = -\frac{qv}{2\Omega\ell} F(\xi,\eta;\beta)$$

$$+ \frac{8qc}{\Omega\ell} \sum_{n=1,3,5\cdots} (-)^{(n-1)/2} K_o[n\pi\eta/(\gamma\beta)] \sin\{[n\pi(1+\beta)/(2\beta)] - \epsilon_n/(2\beta)\}$$

$$e^{-\delta_n\xi/\beta} \cos[n\pi\xi/\beta - n\pi(1+\beta)/(2\beta) - (2\xi-1)\epsilon_n/(2\beta)], \quad \xi > 1 \quad (t > \ell/v) \tag{42}$$

where, again, F is given by (35), $\delta_n = \ell\alpha_n/c$, and $\epsilon_n = \ell\beta_n/c$.

It is worthwhile to summarize the results in (a), (b) and (c) for the three different time intervals. At the midpoint $(z = \ell/2)$ of the wire it is found that the induced current is given by

$$I(\ell/2,t)$$

$$= -\frac{qv}{2\Omega\ell} F(\xi,\eta;\beta), \qquad \xi < 0 \qquad (t < 0) \tag{35}$$

$$= -\frac{qv}{2\Omega\ell} F(\xi,\eta;\beta) + \frac{qv}{2\Omega\ell}\frac{8}{\beta} \sum_{n=1,2,5\cdots} (-)^{(n-1)/2} K_o[n\pi\eta/(\gamma\beta)] e^{-\delta_n\xi/\beta} \sin[(n\pi-\epsilon_n)\xi/\beta]$$

$$0 < \xi < 1 \quad (0 < t < \ell/v) \tag{40}$$

$$= -\frac{qv}{2\Omega\ell} F(\xi,\eta;\beta)$$

$$+ \frac{qv}{2\Omega\ell}\frac{16}{\beta} \sum_{n=1,3,5\cdots} (-)^{(n-1)/2} K_o[n\pi\eta/(\gamma\beta)] \sin\{[n\pi(1+\beta)-\epsilon_n]/(2\beta)\}$$

$$e^{-\delta_n\xi/\beta} \cos[n\pi\xi/\beta - n\pi(1+\beta)/(2\beta) - (2\xi-1)\epsilon_n/(2\beta)], \quad \xi > 1 \quad (t > \ell/v) \tag{42}$$

where $\delta_n = \ell\alpha_n/c$, $\epsilon_n = \ell\beta_n/c$, $\xi = vt/\ell$, $\eta = \rho_o/\ell$, $\beta = v/c$ and

$$F(\xi,\eta;\beta) = \frac{2}{\sqrt{(\eta/\gamma)^2+(\xi-1/2)^2}} - \int_0^\infty \frac{e^{-|\xi|x}+e^{-|1-\xi|x}}{\cosh(\beta x/2)} J_o(\eta x/\gamma)dx \tag{35}$$

$$= \frac{2}{\sqrt{\eta^2+(\xi-1/2)^2}} - \frac{1}{\sqrt{\eta^2+\xi^2}} - \frac{1}{\sqrt{\eta^2+(\xi-1)^2}} + O(\beta^2). \tag{36}$$

The correction term $O(\beta^2)$ in (36) is negligible except when the particle is close to the end points of the wire.

In Table I the damping constant δ_n and the phase shift ε_n are given for each mode in expressions (40) and (42). Figures 8a through 8e give the

Table I

n	$\Omega\delta_n$	$\Omega\varepsilon_n$
1	2.4209	1.4164
3	3.4993	1.5199
5	4.0088	1.5431
7	4.3456	1.5541
9	4.5977	1.5608
11	4.7995	1.5654

variation of $K_o[n\pi\eta/(\gamma\beta)]$ with β for each n and η. These figures together with Table I show the relative importance of the resonant modes excited by a moving charged particle.

In Figs. 9a through 9e the time history of the induced current at the midpoint of the wire as given by (35), (40) and (42) is plotted with β and η as parameters. Note that the time coordinate is expressed in terms of the normalized variable ξ $(=vt/\ell)$, and that the instant $t = 0$ means that the charged particle just reaches a point right above one end of the wire. It is seen that oscillations are being excited when the charge is moving above the wire and continue to sustain themselves with small dampings long after the charge has passed. Superimposed on these figures is the corresponding quasi-static

result given by (16), so that validity criteria for the quasi-static approach can be read off by direct observations. The general conclusion is that the larger the quantity η becomes in comparison to $\beta\gamma$, the better the quasi-static solution is. From the viewpoint of system vulnerability the important conclusion is that resonances of a structure not only introduce rapid oscillations in the induced currents that will last long after the transient source has disappeared but also may significantly increase the peak values of the induced currents. Before concluding it should be pointed out that the parameter η must satisfy the inequality $\eta > \exp(-\Omega/2)$, so that the charged particle is outside the wire; for $\Omega = 10$, $\eta > 0.027$.

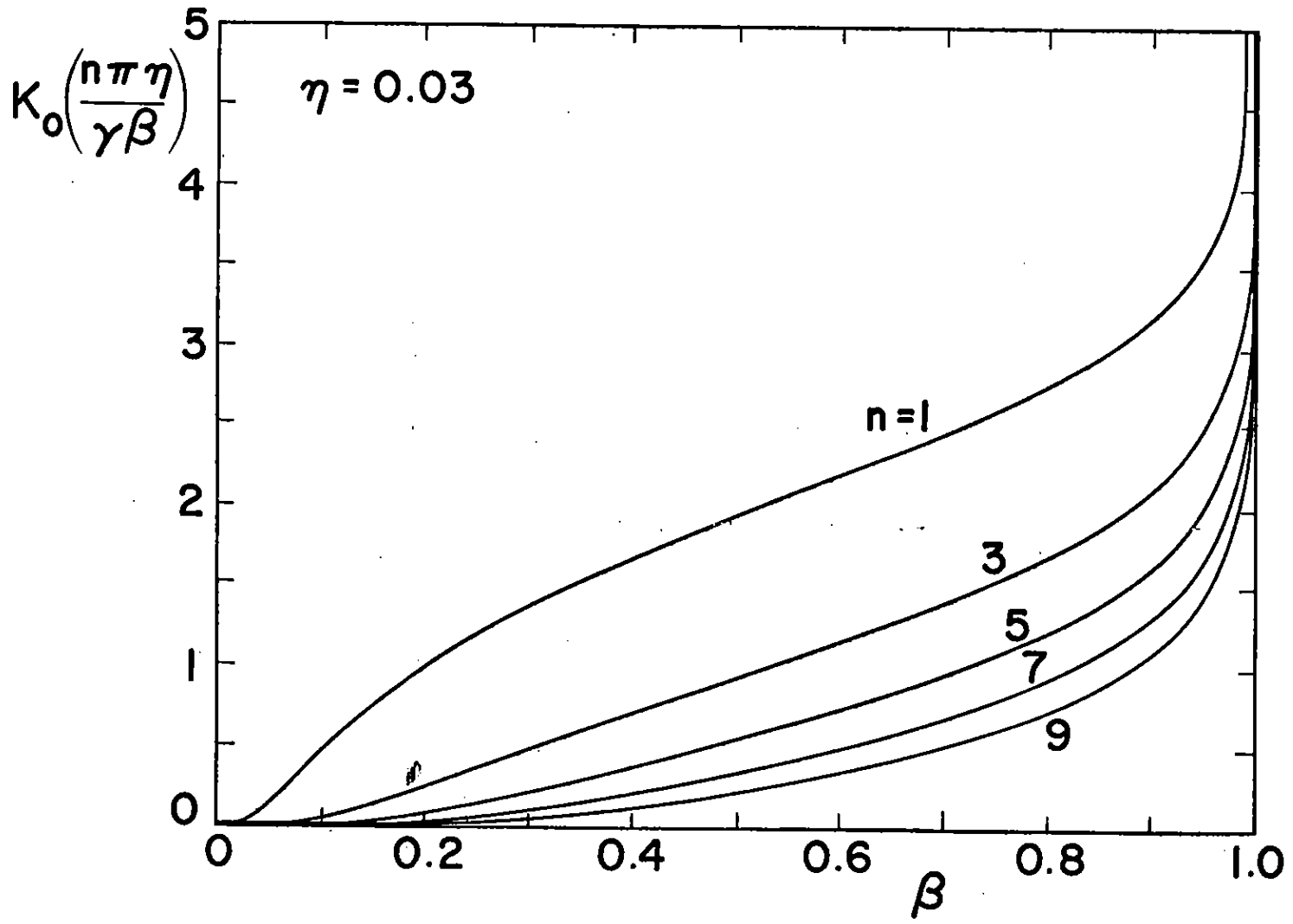

Figure 8a. Variation of excitation coefficient with β for $\eta = 0.03$.

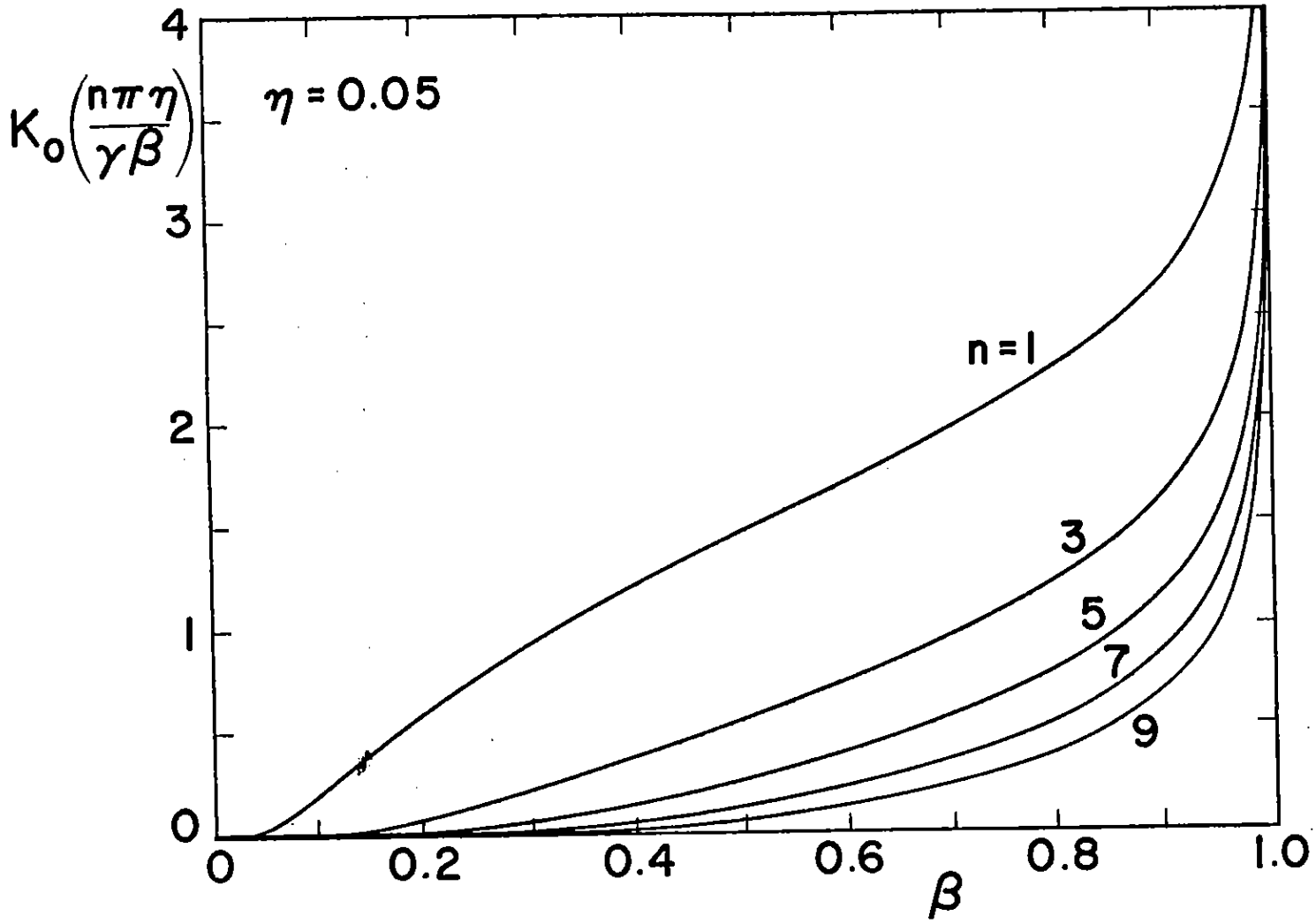

Figure 8b. Variation of excitation coefficient with β for $\eta = 0.05$.

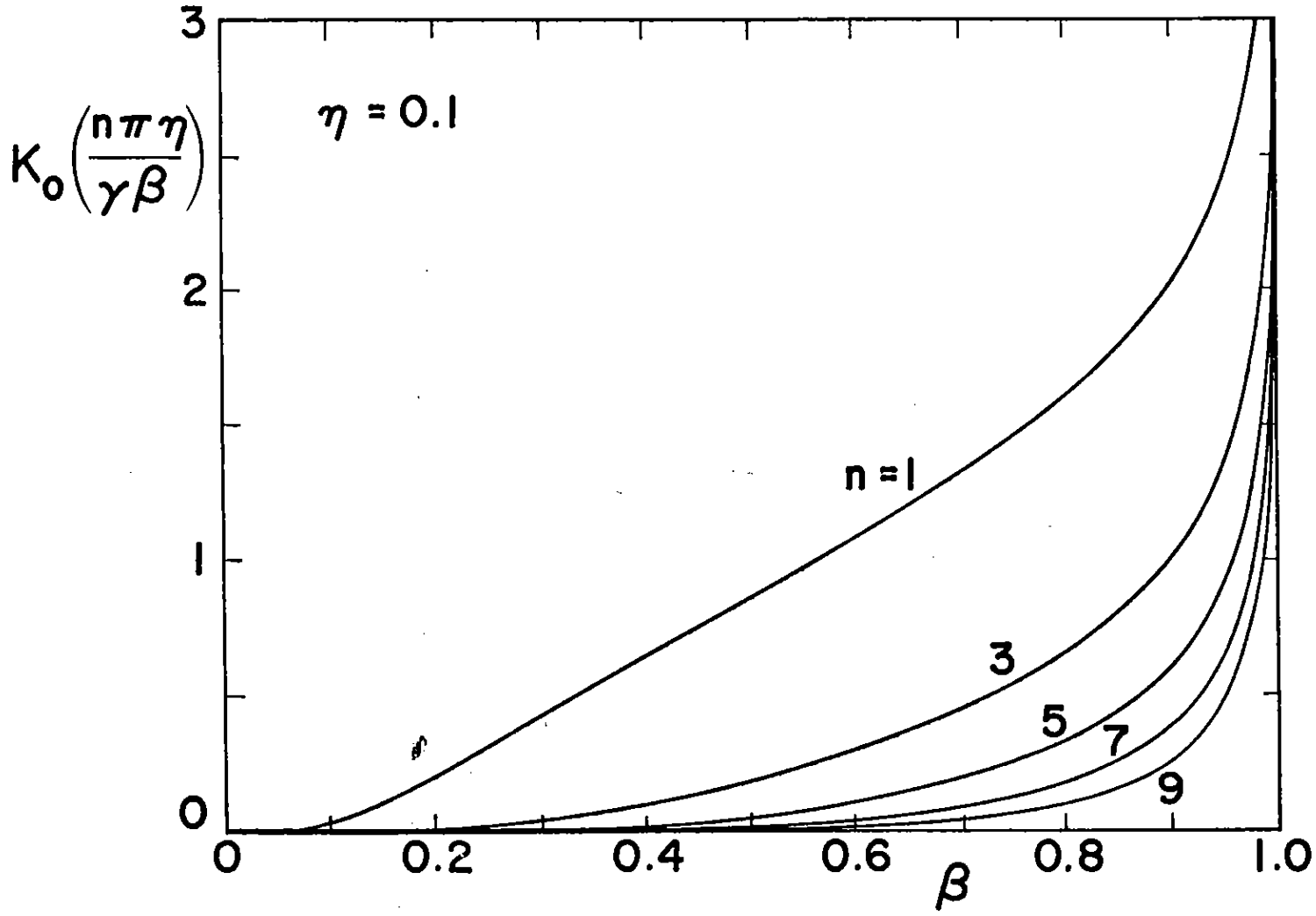

Figure 8c. Variation of excitation coefficient with β for $\bar{\eta} = 0.1$.

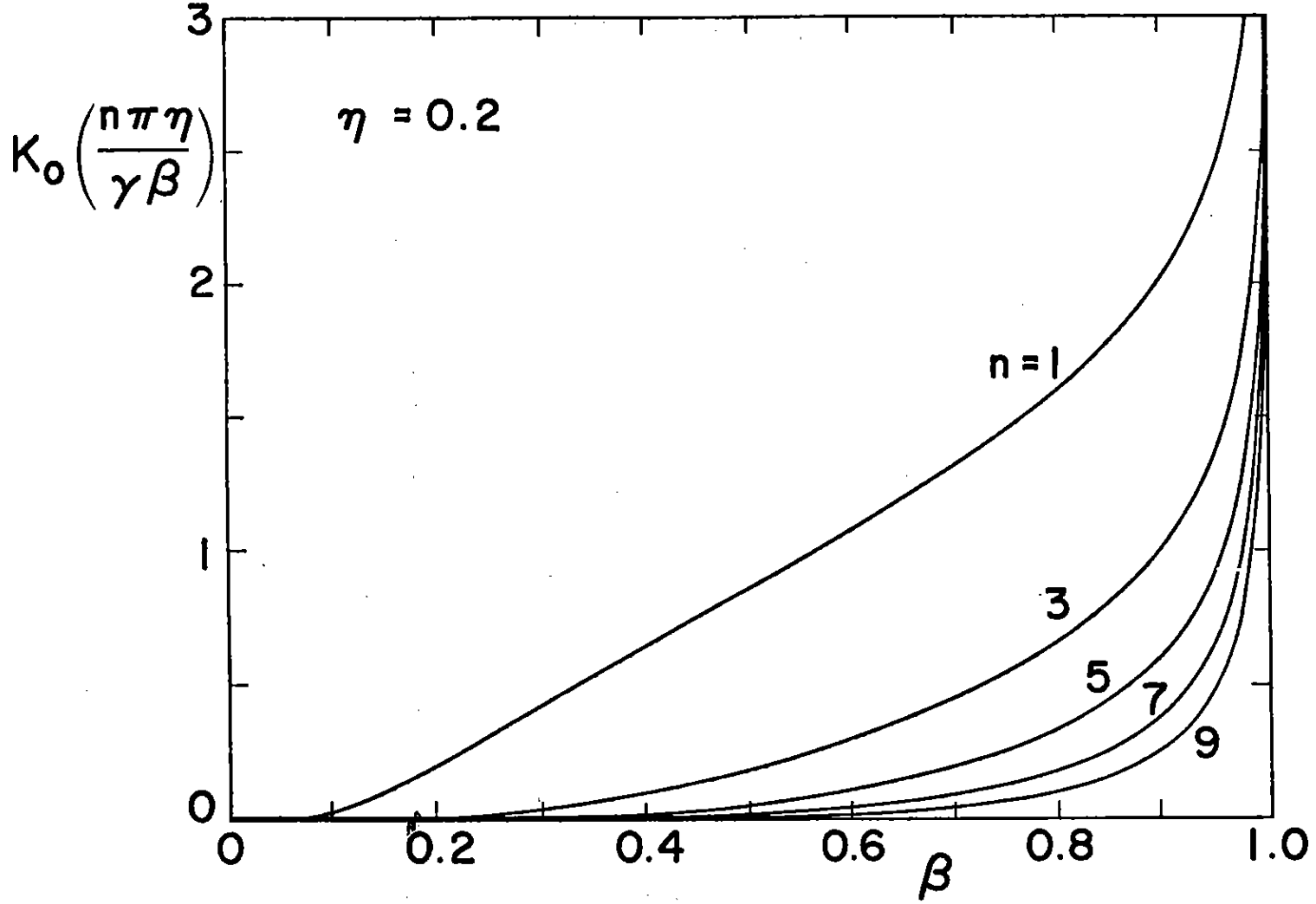

Figure 8d. Variation of excitation coefficient with β for $\eta = 0.2$.

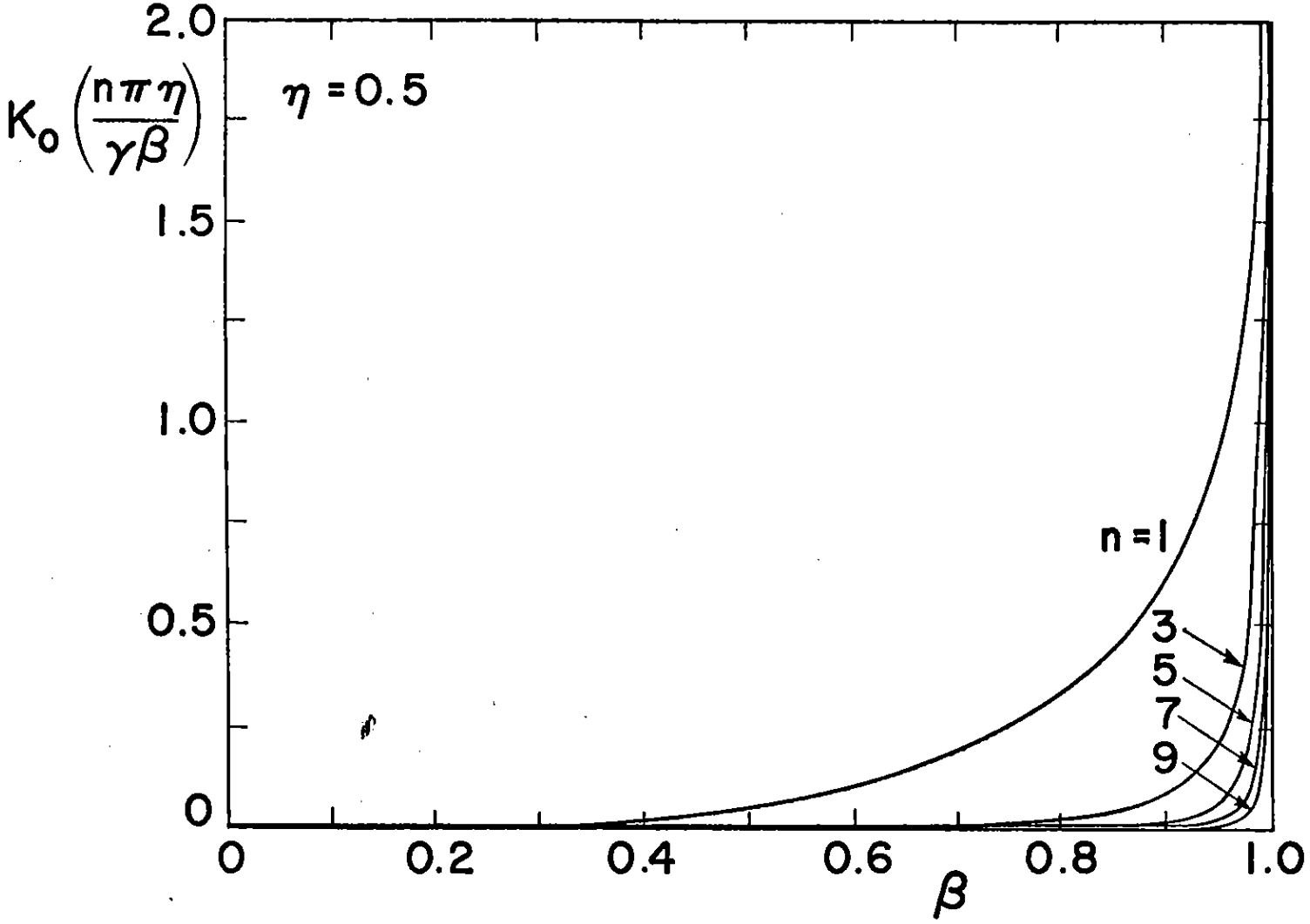

Figure 8e. Variation of excitation coefficient with β for $\eta = 0.5$.

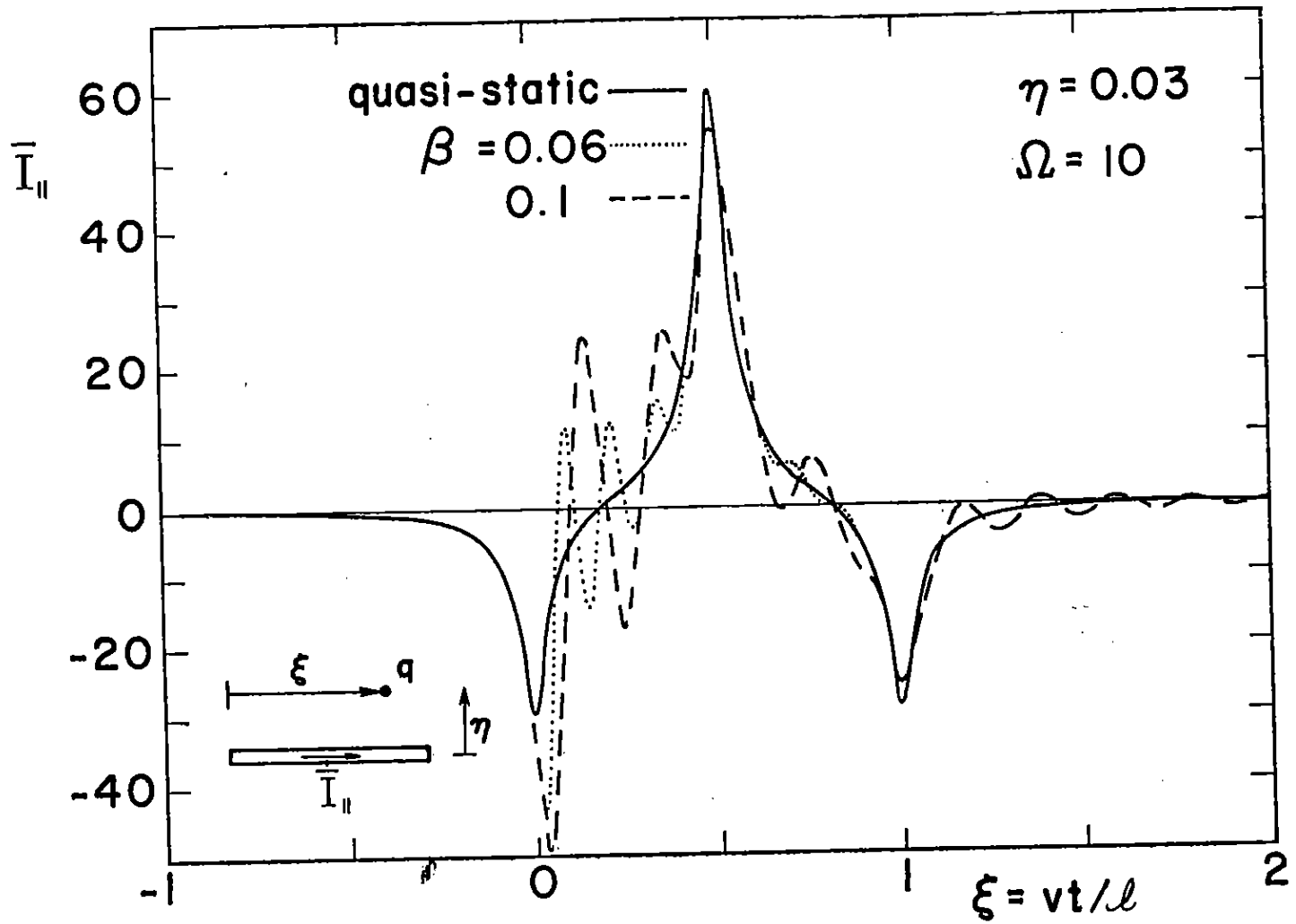

Figure 9a. Time history of induced current at the wire midpoint for $\eta = 0.03$.

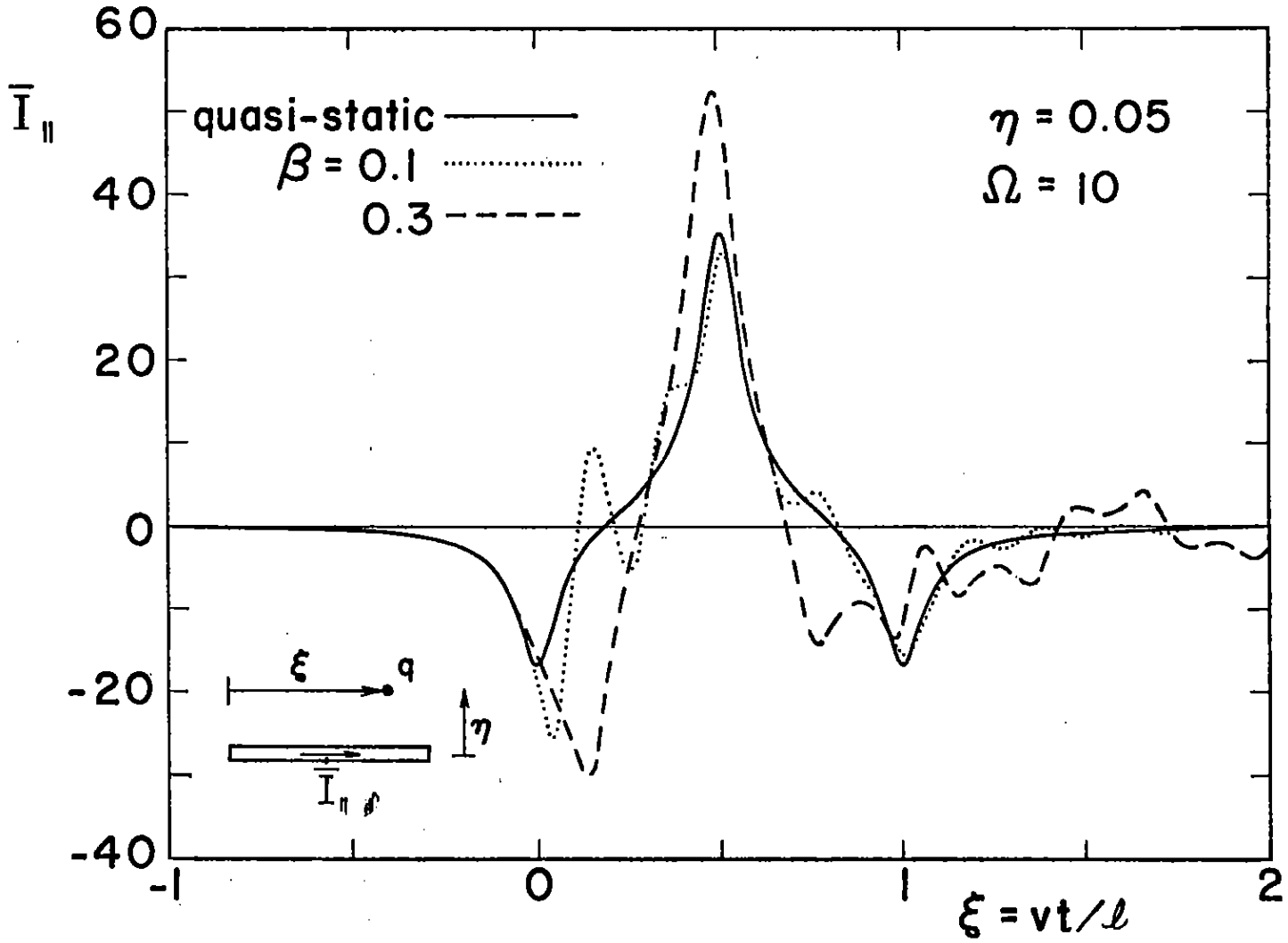

Figure 9b. Time history of induced current at the wire midpoint for $\eta = 0.05$.

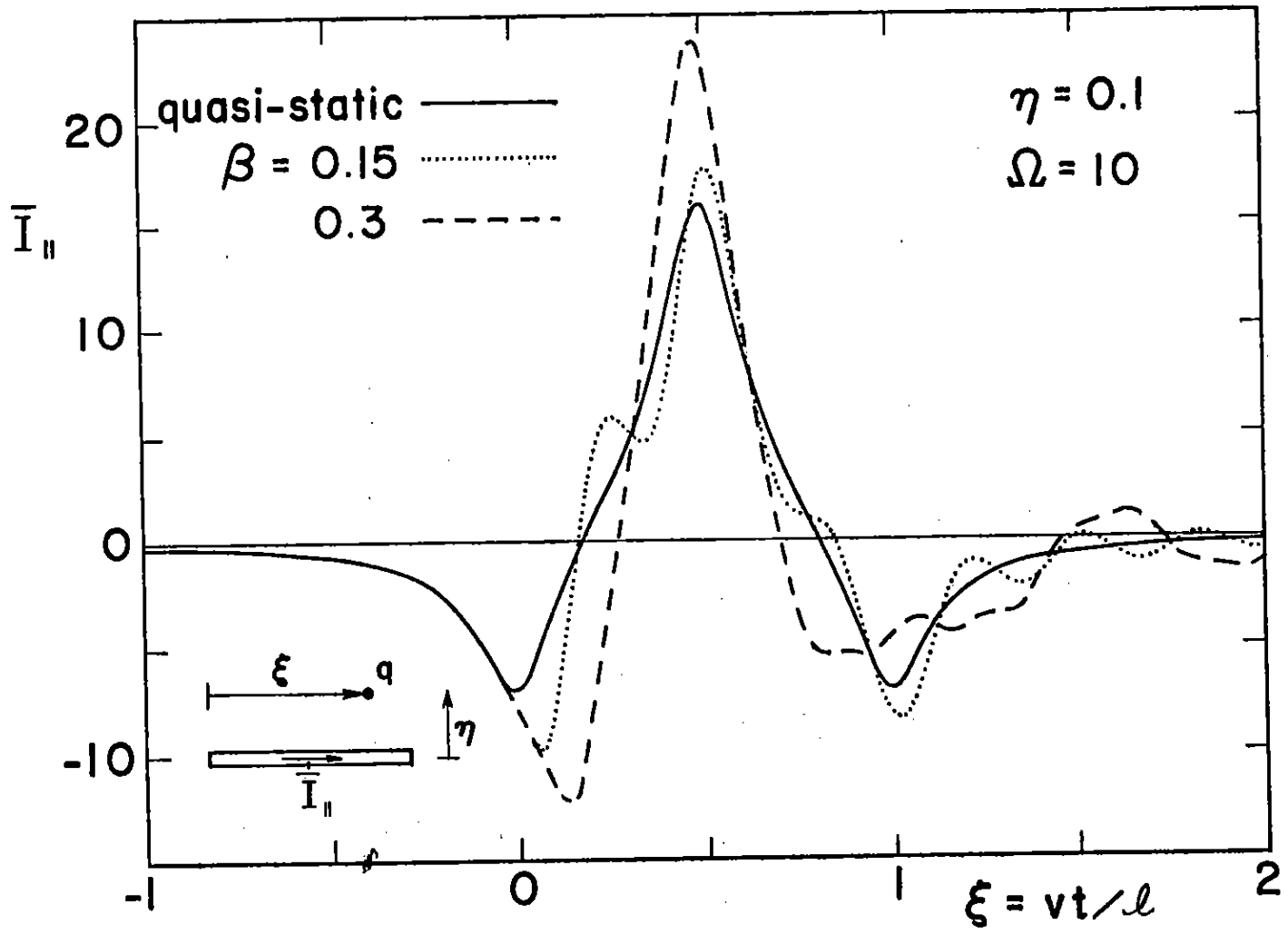

Figure 9c. Time history of induced current at the wire midpoint for $\eta = 0.1$.

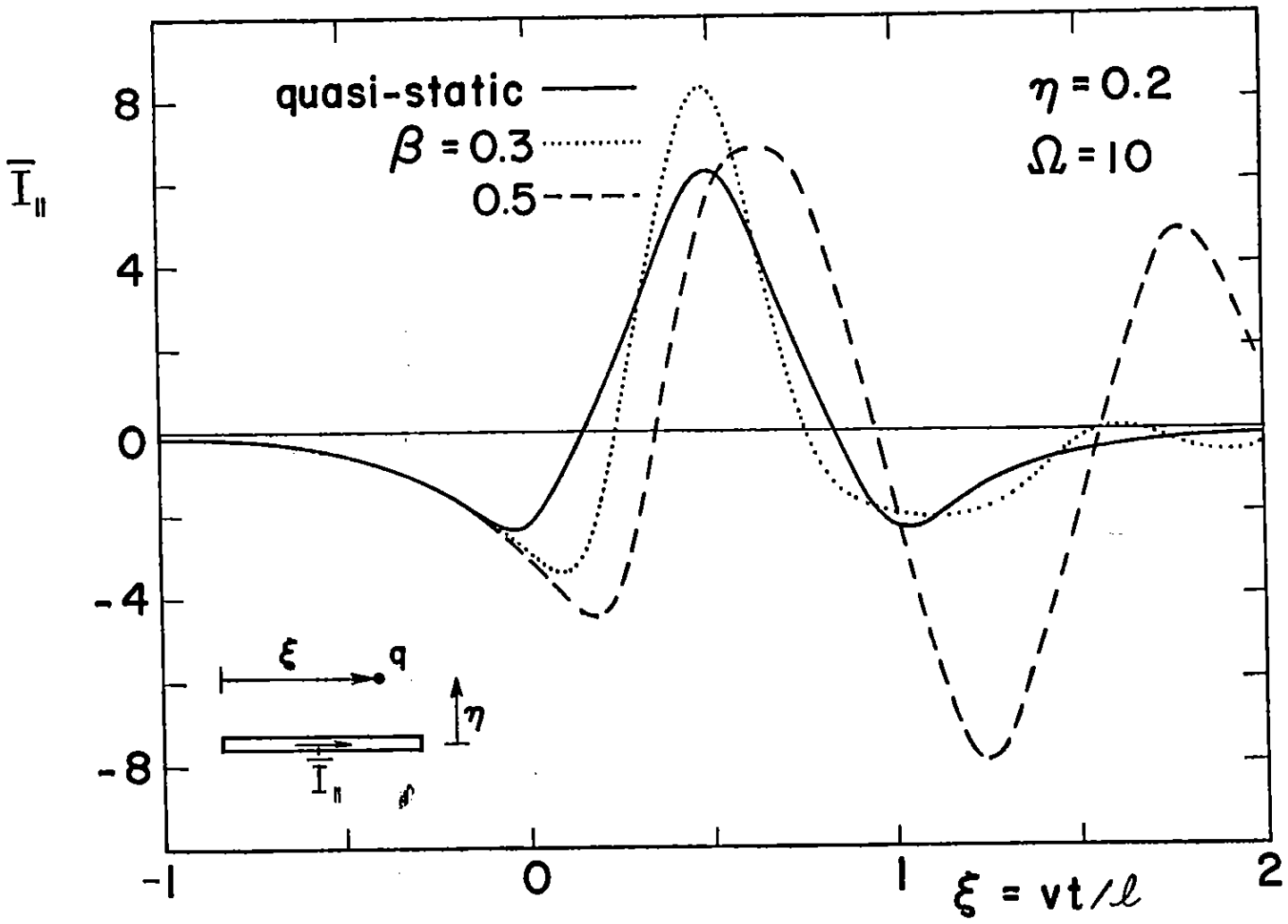

Figure 9d. Time history of induced current at the wire midpoint for $\eta = 0.2$.

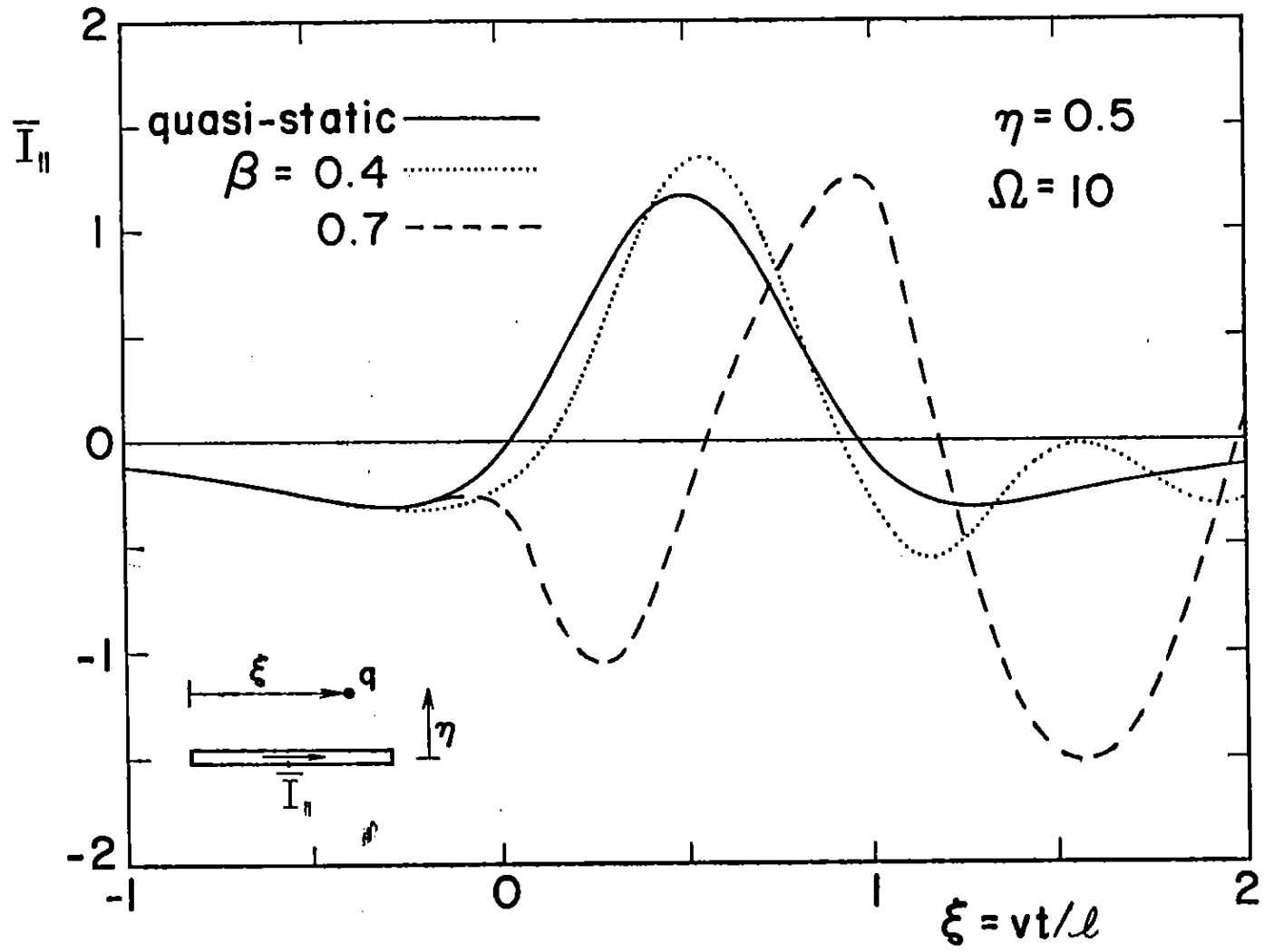

Figure 9e. Time history of induced current at the wire midpoint for $\eta = 0.5$.

IV. Space-Time Integral Formulation

In the preceding section the method of natural modes together with an asymptotic expansion was used to solve the differential-integral equation that governs the induced current on the wire. By treating Ω as a large expansion parameter it was possible to write the induced current into two parts: one part consists of damped sinusoids and the other part has the quasi-static behavior. In this section, the analytical solution for the induced current obtained in the last section will be checked against the numerical solution of an exact formulation without an asymptotic expansion in large Ω. The reason to do this is that the method presented in the last section not only has many attractive features but also can be extended to other more elaborate models of a satellite; therefore, it is highly desirable to establish the domain of its validity.

The starting point is the inverse Laplace transform of (17), i.e.,

$$\left(\frac{\partial^2}{\partial z^2} - \frac{1}{c^2}\frac{\partial^2}{\partial t^2}\right)\int_0^{\ell} \frac{I(z',t-|z-z'|/c)}{4\pi\sqrt{a^2+(z-z')^2}}\,dz' = -\epsilon\frac{\partial}{\partial t}E_z^{inc}. \tag{43}$$

To solve this equation one can invoke the one-dimensional retarded Green's function

$$G(z,t;z',t') = \frac{c}{2}U(t - t' - |z - z'|/c) \tag{44}$$

which, of course, satisfies the differential equation

$$\left(\frac{\partial^2}{\partial z^2} - \frac{1}{c^2}\frac{\partial^2}{\partial t^2}\right)G = -\delta(z - z')\delta(t - t'). \tag{45}$$

In (44), U is the unit-step function. Now, one can immediately write down the solution to (43) as

$$\frac{1}{4\pi}\int_0^{\ell}\frac{I(z',t-|z-z'|/c)}{\sqrt{a^2+(z-z')^2}}\,dz' = f_1(ct - z) + f_2(ct + z) + \frac{1}{2Z_o}\int_0^{\ell}\int_{-\infty}^{\infty}\frac{\partial E_z^{inc}}{\partial t'}U(t - t' - |z - z'|/c)dt'dz'$$

where Z_o is the free-space wave impedance. Carrying out the t' integration one finally gets

$$\frac{1}{4\pi}\int_0^{\ell}\frac{I(z',t-|z-z'|/c)}{\sqrt{a^2+(z-z')^2}}\,dz' = f_1(ct-z)+f_2(ct+z) + \frac{1}{2Z_o}\int_0^{\ell}E_z^{inc}(z',t-|z-z'|/c)dz' \qquad (46)$$

where f_1 and f_2 are arbitrary functions which will be determined by the end conditions that $I(\ell,t) = I(0,t) = 0$. Equation (46) has been derived before and numerically solved for some simple incident electric fields [12]. In the present case, E_z^{inc} is due to a moving charge with an infinite path; that is to say, there are no zero initial conditions which are, however, implicit in (46). This difficulty can be remedied by shifting the time origin sufficiently into the past so that the initial conditions with respect to the new time origin are almost zero. With this modification (46) was solved on an electronic computer and the numerical results are presented in Figs. 10a through 12b for some selective values of β and η together with the corresponding results obtained in the last section. As expected, the larger the value Ω becomes the more closely the asymptotic solution agrees with the numerical solution of (46). It is observed that the two solutions give almost the same wave shapes. For the smallest Ω value in these figures, i.e., $\Omega = 10$, the asymptotic solution is smaller than the numerical solution of (46) by a factor less than two. It has to be pointed out that for small values of η and/or β, an inordinate amount of computer time would be required to get a satisfactory numerical solution. Hence, one may conclude that for $\Omega \geq 10$ the asymptotic solution is adequate for the prediction of SGEMP induced currents. Before concluding this section, it should be emphasized again that the method of solution presented in Section III, which leads to the asymptotic solution, is preferrable to a brute-force numerical method, since the former is not only much simpler computationally but also provides solutions that can be physically interpreted.

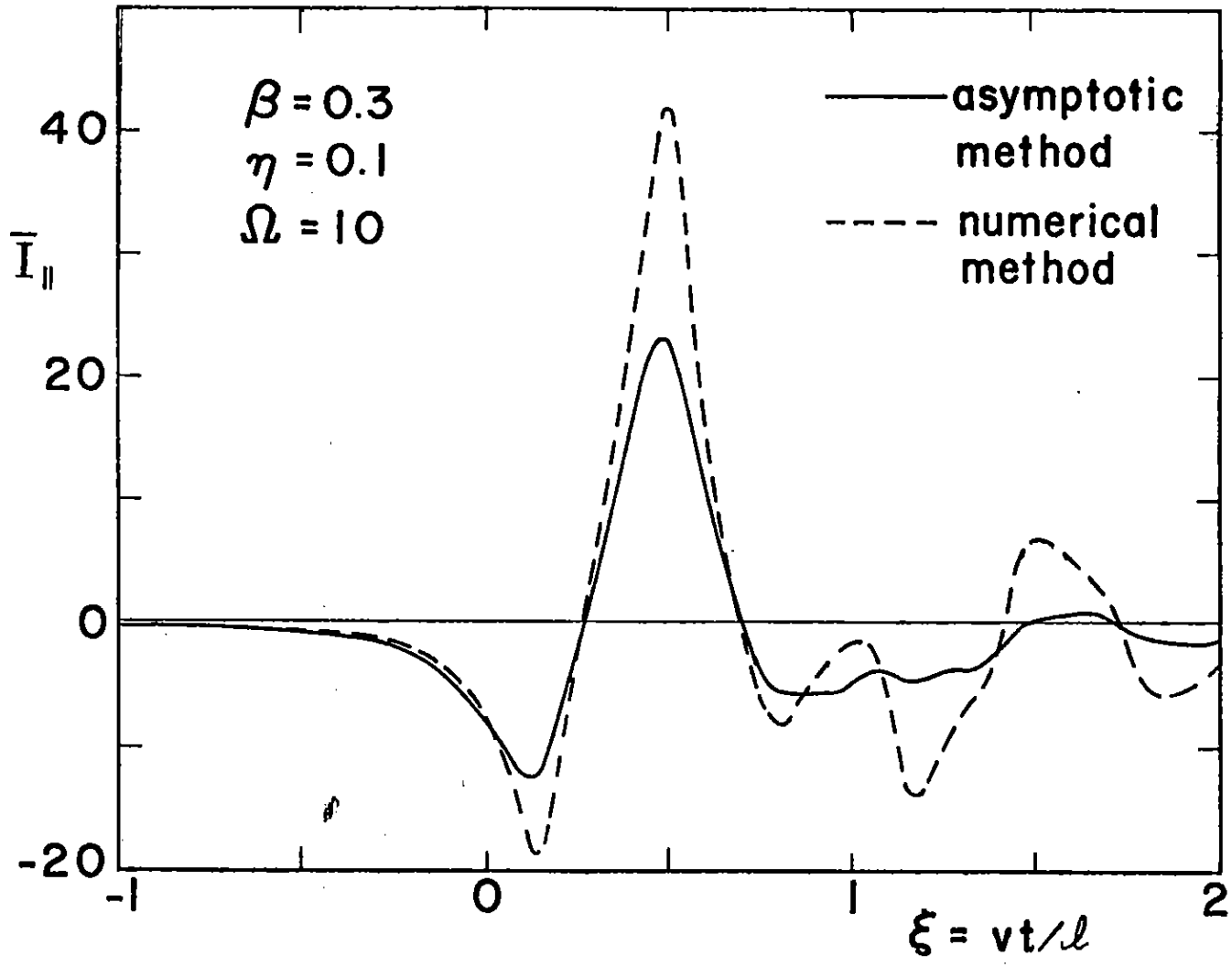

Figure 10a. Comparison between natural mode asymptotic solution [eq.(35),(40),(42)] and numerical solution of eq.(46) for $\Omega = 10$.

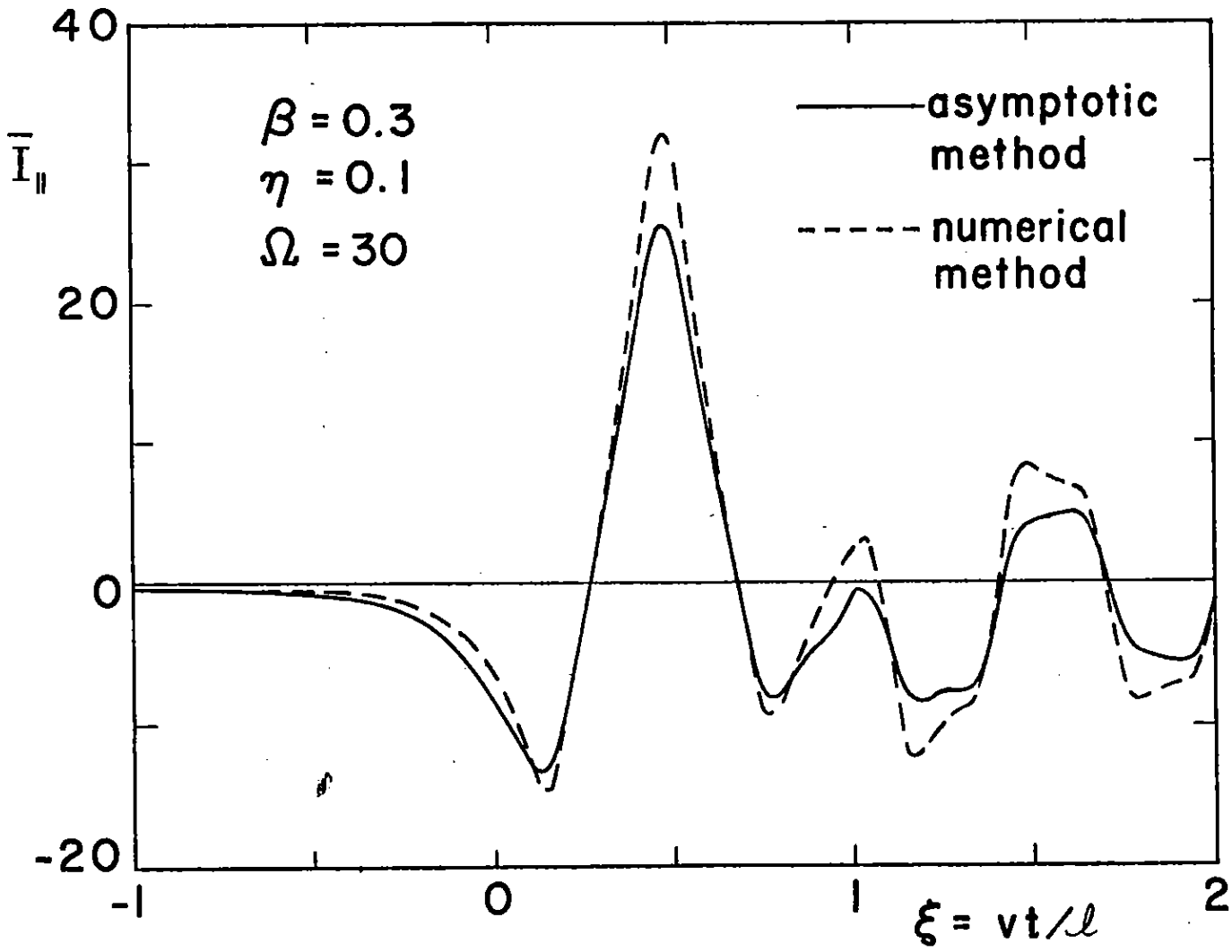

Figure 10b. Comparison between natural mode asymptotic solution [eq.(35),(40),42)] and numerical solution of eq.(46) for $\Omega = 30$.

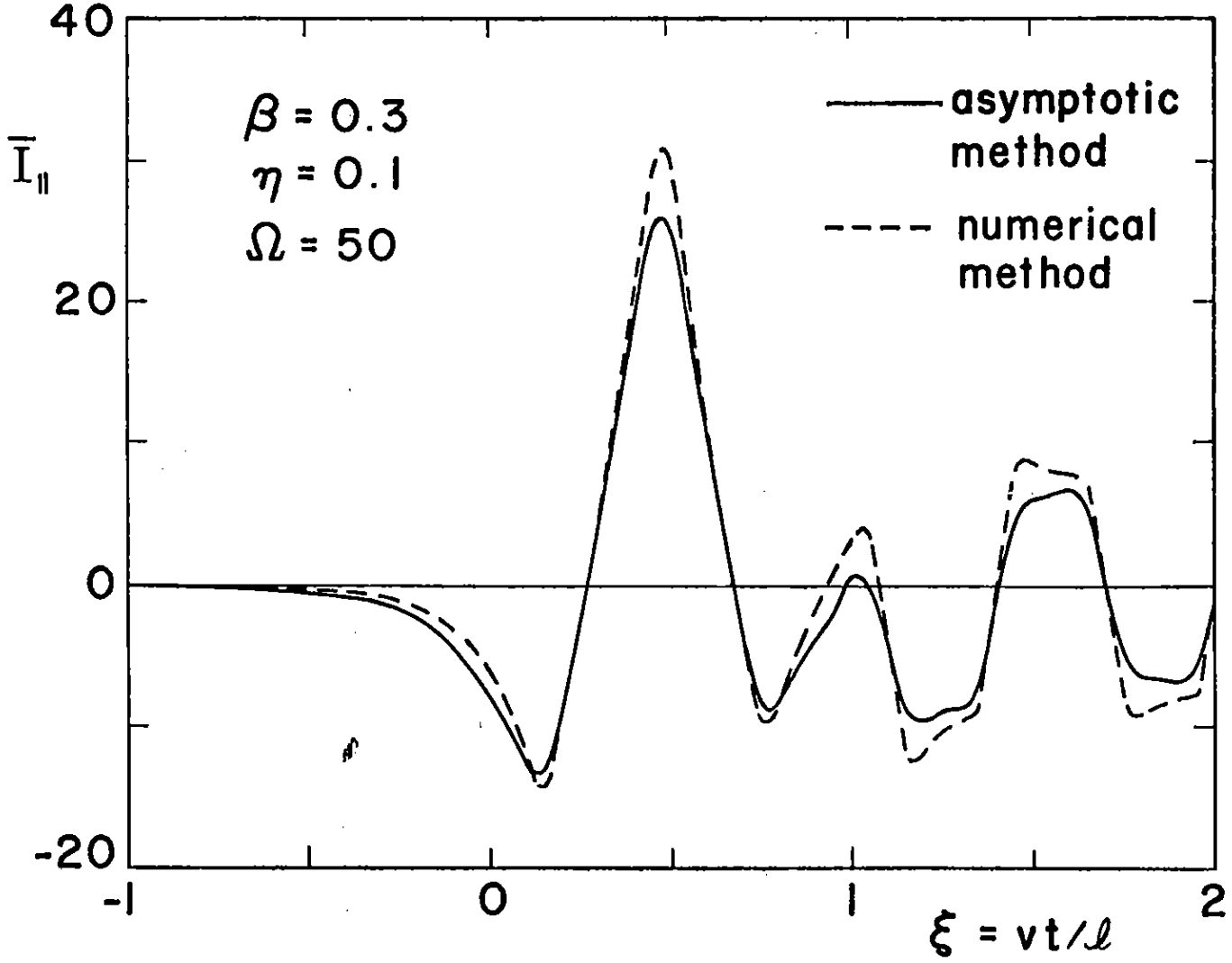

Figure 10c. Comparison between natural mode asymptotic solution [eq.(35),(40),(42)] and numerical solution of eq.(46) for $\Omega = 50$.

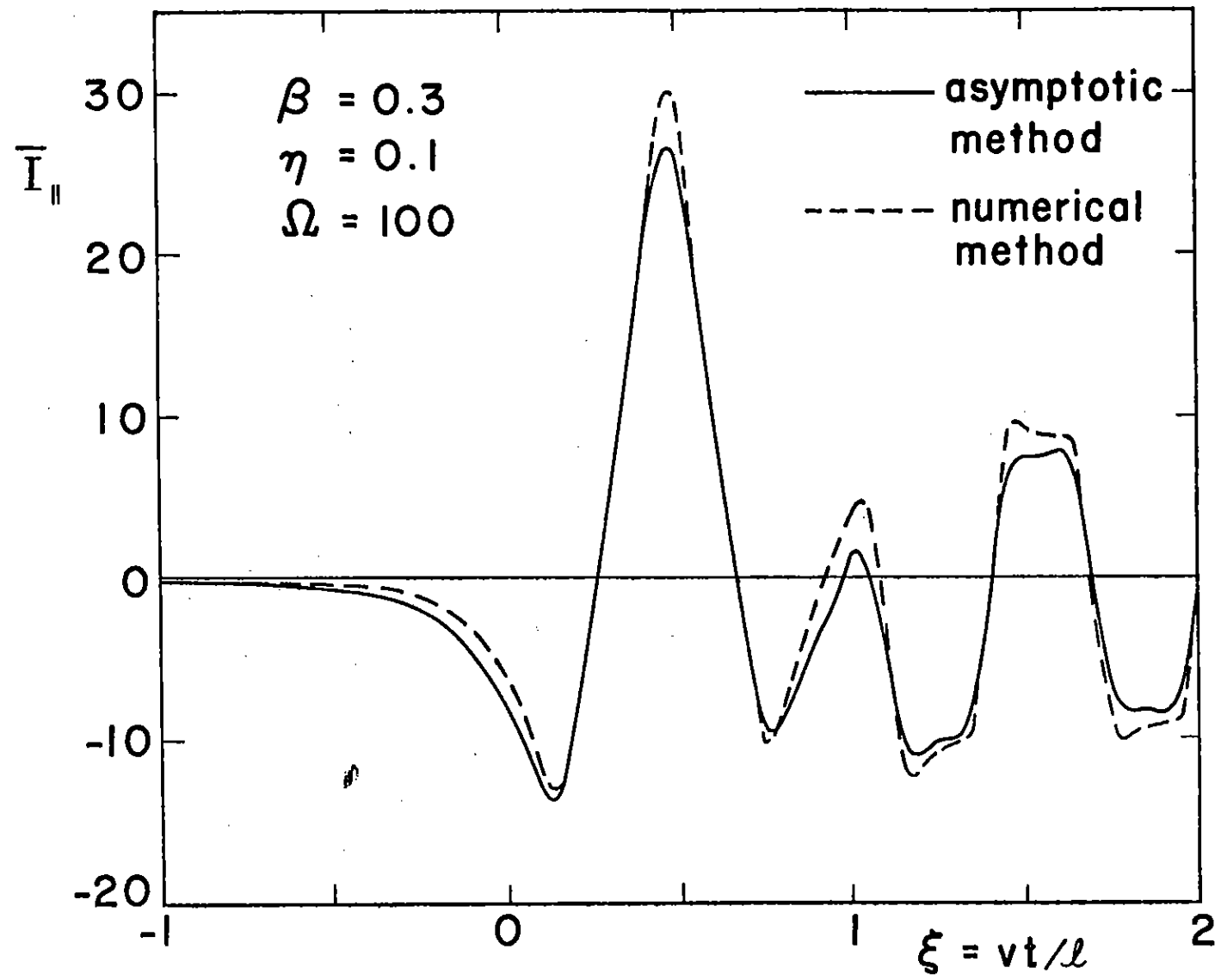

Figure 10d. Comparison between natural mode asymptotic solution [eq.(35),(40),(42)] and numerical solution of eq.(46) for $\Omega = 100$.

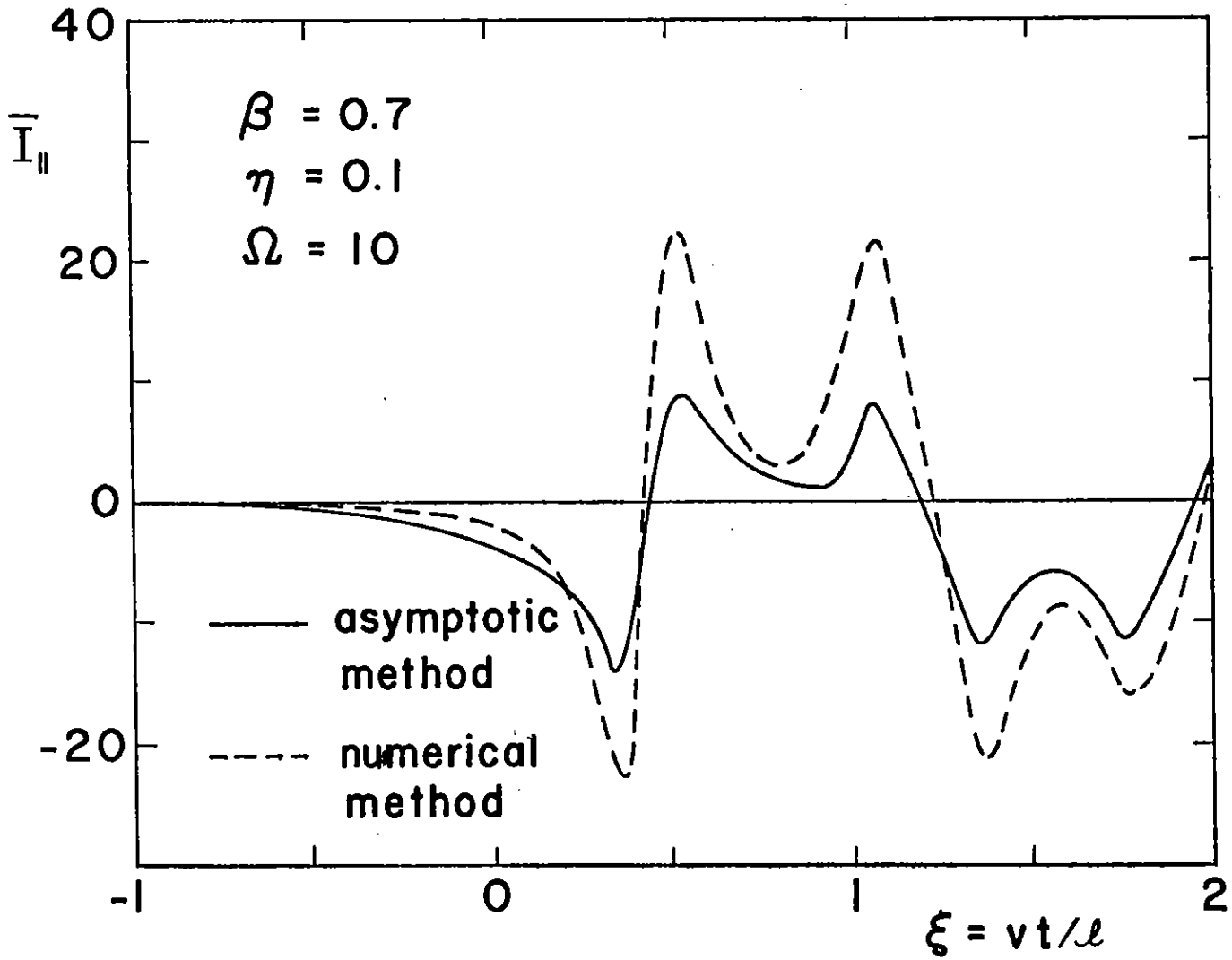

Figure 11a. Comparison between the two solutions at higher velocity for $\Omega = 10$.

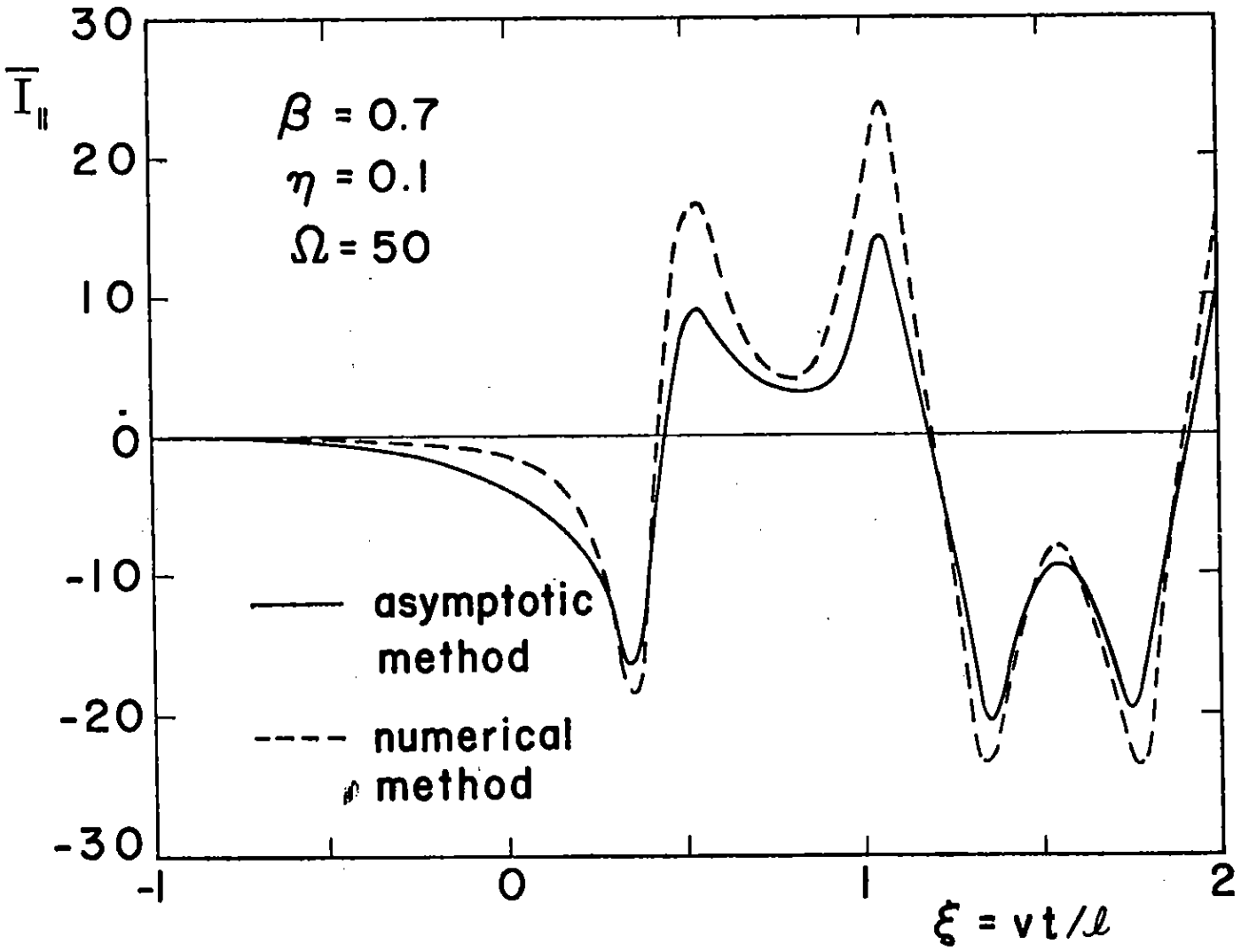

Figure 11b. Comparison between the two solutions at higher velocity for $\Omega = 50$.

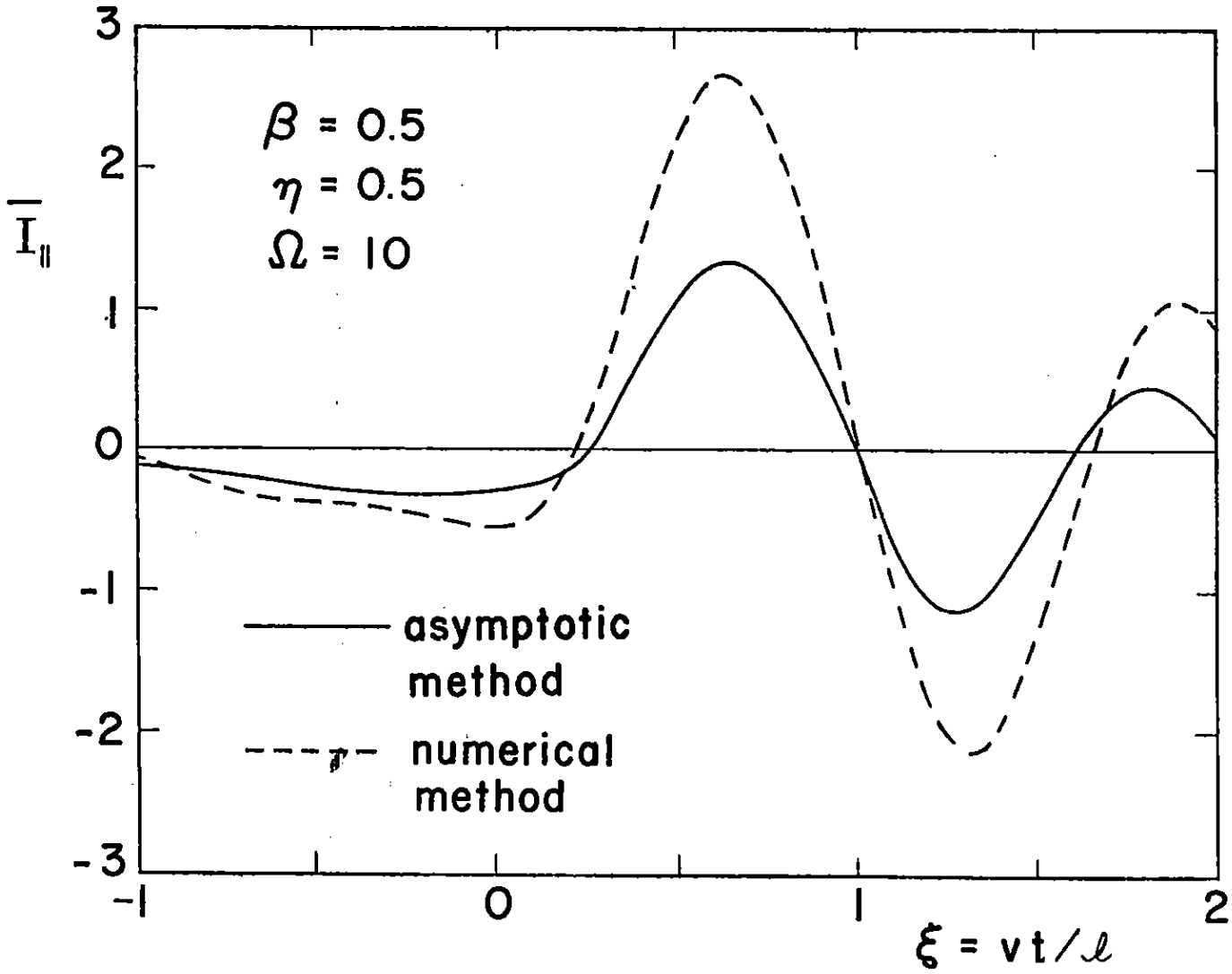

Figure 12a. Comparison between the two solutions for larger particle distance and $\Omega = 10$.

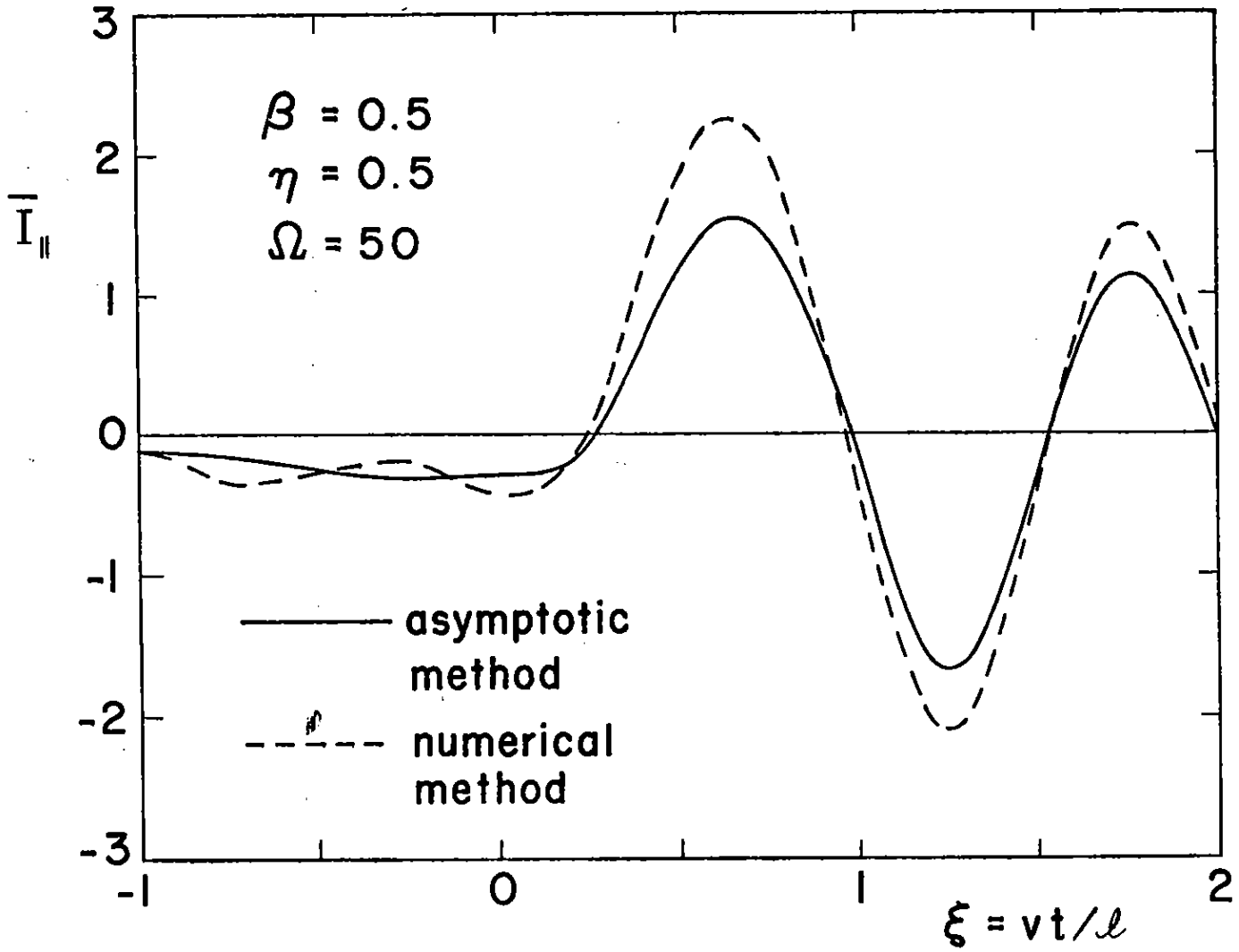

Figure 12b. Comparison between the two solutions for larger particle distance and $\Omega = 50$.

V. Summary and Conclusion

The time history of the current on a wire induced by a moving charged particle is obtained by three different approaches: (1) quasi-static approach, (2) natural-mode approach, and (3) space-time-integral-equation approach. By comparing the results deduced from the three approaches the accuracy of the results and the ranges of validity can be established for each method of solution.

It is found that

(a) for $\eta \leq 0.1$ and $\beta \leq 0.1$ (about 2.6 Kev for electrons) the quasi-static solution is quite good and the transient solution oscillates about the quasi-static solution (see Figs.9a-9c);

(b) for $\eta > 0.1$ the peak value of the induced current obtained by the quasi-static approach agrees very well with that calculated by the natural-mode approach;

(c) the larger the value of β is, the larger the oscillations will be in the induced current waveform, especially after the particle has passed (or "disappeared") the wire;

(d) the natural-mode approach gives an accurate time variation of the induced current; the peak current value calculated from this approach agrees more closely with the "true" value as Ω is increased; for $\Omega = 10$ or so the peak value is within a factor less than two (the Ω value of a typical satellite is about 15 or so);

(e) the space-time-integral-equation approach, although exact, is entirely numerical and applies only to thin wires.

It is concluded that the most promising method for calculating SGEMP induced currents on resonant structures appears to be the natural-mode approach in conjunction with the method of asymptotic expansion. This approach enables one to get an explicit analytic solution which can be interpreted physically with great ease. When other features of a communications satellite, such as the solar panels and the impedance loading the center of the boom (Fig.1), are added to the thin wire considered in this note, the natural-mode approach seems to be the most appealing one because these added features are expected to enhance the resonance effects.

Acknowledgment

Thanks go to Capt. Bob Gardner and Dr. Carl Baum for their interest and useful suggestions in the work. The authors are greatly indebted to Dr. Tom Liu for his help in preparing the material and providing illuminating discussions.

References

1. Baum, C.E., "A Technique for Simulating the System Generated Electromagnetic Pulse Resulting From an Exoatmospheric Nuclear Weapon Radiation Environment," Sensor and Simulation Notes, 156, September 1972.
2. Longmire, C.L., "External System Generated EMP on Some Types of Satellite Structures," Theoretical Notes, 124, August 1971.
3. Lee, K.S.H. and Marin, L., "Interaction of External System-Generated EMP With Space Systems," Theoretical Notes, 179, August 1973.
4. Gardner, R.L., "The Electromagnetic Fields due to Radial Currents Near a Perfectly Conducting Sphere," MS Thesis, unpublished, Air Force Institute of Technology, March 1973.
5. Marin, L., "Natural Modes of Certain Thin-Wire Structures," Interaction Notes, 186, August 1974.
6. Landau, L.D. and Liftshitz, E.M., Electrodynamics of Continuous Media, Pergamon Press, New York, 1960.
7. Baum, C.E., "On the Singularity Expansion Method for the Case of First Order Poles," Interaction Notes, 129, October 1972.
8. Hallén, E., "Theoretical Investigations Into the Transmitting and Receiving Qualities of Antennae," Nova Acta Reg. Soc. Sci. Upsaliensis, 11, No. 4, pp. 1-44, 1938.
9. Gradshteyn, I.S. and Ryzhik, I.W., Table of Integrals, Series and Products, Academic Press, New York, 1965.
10. Jackson, J.D., Classical Electrodynamics, John Wiley, New York, 1962.
11. Erdélyi, A., Editor, Tables of Integral Transforms, Vol. 1, McGraw-Hill, New York, 1954.
12. Liu, T.K., "Direct Time Domain Analysis of Linear EMP Radiators," Sensor and Simulation Notes, 154, July 1972.